Recent increases in the atmospheric growth rate and emissions of HFC-23 (CHF_3) and the link to HCFC-22 ($CHClF_2$) production

Peter G. Simmonds[1], Matthew Rigby[1], Archie McCulloch[1], Martin K. Vollmer[2], Stephan Henne[2], Jens Mühle[3], Simon O'Doherty[1], Alistair J. Manning[4], Paul B. Krummel[5], Paul J. Fraser[5], Dickon Young[1], Ray F. Weiss[3], Peter K. Salameh[3], Christina M. Harth[3], Stefan Reimann[2], Cathy M. Trudinger[5], L. Paul Steele[5], Ray H. J. Wang[6], Diane J. Ivy[7], Ronald G. Prinn[7], Blagoj Mitrevski[5], and David M. Etheridge[5].

[1] Atmospheric Chemistry Research Group, University of Bristol, Bristol, UK
[2] Swiss Federal Laboratories for Materials Science and Technology, Laboratory for Air Pollution and Environmental Technology (Empa), Dübendorf, Switzerland,
[3] Scripps Institution of Oceanography (SIO), University of California at San Diego, La Jolla, California, USA
[4] Met Office Hadley Centre, Exeter, UK
[5] Climate Science Centre, Commonwealth Scientific and Industrial Research Organisation (CSIRO) Oceans and Atmosphere, Aspendale, Victoria, Australia
[6] School of Earth, and Atmospheric Sciences, Georgia Institute of Technology, Atlanta, Georgia, USA
[7] Center for Global Change Science, Massachusetts Institute of Technology, Cambridge, Massachusetts, USA

Correspondence to: P.G. Simmonds (petergsimmonds@aol.com)

Abstract

High frequency measurements of trifluoromethane (HFC-23, CHF_3), a potent hydrofluorocarbon greenhouse gas, largely emitted to the atmosphere as by-product of production of the hydrochlorofluorocarbon HCFC-22 ($CHClF_2$), at five core stations of the Advanced Global Atmospheric Gases Experiment (AGAGE) network, combined with measurements on firn air, old Northern Hemisphere air samples and Cape Grim Air Archive (CGAA) air samples, are used to explore the current and historic changes in the atmospheric abundance of HFC-23. These measurements are used in combination with the AGAGE 2-D atmospheric 12-box model and a Bayesian inversion methodology to determine model atmospheric mole fractions and the history of global HFC-23 emissions. The global modelled annual mole fraction of HFC-23 in the background atmosphere was 28.9 ± 0.6 pmol mol^{-1} at the end of 2016, representing a 28% increase from 22.6 ± 0.4 pmol mol^{-1} in 2009. Over the same time frame, the modelled mole fraction of HCFC-22 increased by 19% from 199 ± 2 pmol mol^{-1} to 237 ± 2 pmol mol^{-1}. However, unlike HFC-23, the annual average HCFC-22 growth rate slowed from 2009 to 2016 at an annual average rate of -0.5 pmol mol^{-1} yr^{-2}. This slowing atmospheric growth is consistent with HCFC-22 moving from dispersive (high fractional emissions) to feedstock (low fractional emissions) uses, with HFC-23 emissions remaining as a consequence of incomplete mitigation from all HCFC-22 production.

Our results demonstrate that, following a minimum in HFC-23 global emissions in 2009 of 9.6 ± 0.6 Gg yr^{-1}, emissions increased to a maximum in 2014 of 14.5 ± 0.6 Gg yr^{-1} and then declined to 12.7 ± 0.6 Gg yr^{-1} (157 Mt CO_2-e yr^{-1}) in 2016. The 2009 emissions minimum is consistent with estimates based on national reports and is likely a response to the implementation of the Clean Development Mechanism (CDM) to mitigate HFC-23 emissions by incineration in developing (Non-Annex 1) countries under the Kyoto Protocol. Our derived cumulative emissions of HFC-23 during 2010-2016 were 89 ± 2 Gg (1.1 ± 0.2 Gt CO_2-e), which led to an increase in radiative forcing of 1.0 ± 0.1 mW m^{-2} over the same period. Although the CDM had reduced global HFC-23 emissions, it cannot now offset the higher emissions from increasing HCFC-22 production in Non-Annex 1 countries, as the CDM was closed to new entrants in 2009. We also find that the cumulative European HFC-23 emissions from 2010 to 2016 were ~1.3 Gg, corresponding to just 1.5% of cumulative global HFC-23 emissions over this same period. The majority of the increase in global HFC-23 emissions since 2010 is attributed to a delay in the adoption of mitigation technologies, predominantly in China and east Asia. However, a reduction in emissions is anticipated, when the Kigali 2016 amendment to the Montreal Protocol, requiring HCFC and HFC production facilities to introduce destruction of HFC-23, is fully implemented.

1. Introduction

Due to concerns about climate change, trifluoromethane (CHF_3, HFC-23) has attracted interest as a potent greenhouse gas due to a100-yr integrated global warming potential (GWP) of 12400 (Myhre et al., 2013) and an atmospheric lifetime of ~228 yr (SPARC, 2013). Hydrofluorocarbons (HFCs) were introduced as replacements for ozone-depleting chlorofluorocarbons (CFCs) and hydrochlorofluorocarbons (HCFCs) - for example, HFC-134a as a direct replacement for CFC-12 (Xiang et al., 2014). However, HFC-23 is a by-product of chlorodifluoromethane HCFC-22 ($CHClF_2$) production, resulting from the over-fluorination of chloroform ($CHCl_3$). Most HFC-23 has historically been vented to the atmosphere (UNEP, 2017a). HFC-23 has also been used as a feed-stock in the production of Halon-1301 ($CBrF_3$) (Miller and Batchelor, 2012) which substantially decreased with the phase-out of halons in 2010 under the Montreal Protocol, a landmark international agreement designed to protect the stratospheric ozone layer. HFC-23 also has minor emissive uses in air conditioning, fire extinguishers, and semi-conductor manufacture (McCulloch and Lindley, 2007) and very minor emissions from aluminium production (Fraser et al., 2013). For developed countries HFC-23 emissions were controlled as part of the "F-basket" under the Kyoto Protocol, an international

77 treaty among industrialized nations that sets mandatory limits on greenhouse gas emissions,
78 (https://ec.europa.eu/clima/policies/f-gas_en).

79 In the context of this paper, we discuss "developed" and "developing" countries which
80 we take to be synonymous with Annex 1 (Non-Article 5) countries and Non-Annex 1 (Article 5)
81 countries, respectively.

82 There have been a number of previous publications related to HFC-23. Oram et al.
83 (1998) measured HFC-23 by gas chromatography-mass spectrometry (GC-MS) analysis of Cape
84 Grim flask air samples and sub-samples of the Cape Grim Air Archive (CGAA) from 1978-1995 and
85 reported a dry-air southern hemispheric atmospheric abundance of 11 pmol mol^{-1} in late-1995.
86 Culbertson et al. (2004) estimated global emissions of HFC-23 using a one-box model and GC-MS
87 analysis of north American and Antarctic air samples. A top-down HFC-23 emissions history and a
88 comprehensive bottom-up estimate of global HFC-23 emissions were reported by Miller et al.
89 (2010) using Advanced Global Atmospheric Gases Experiment (AGAGE) observations (2007-
90 2009) and samples from the CGAA (1978-2009). Montzka et al. (2010), using measurements of
91 firn air from the permeable upper layer of an ice sheet and ambient air collected during three
92 expeditions to Antarctica between 2001 and 2009, constructed a consistent Southern Hemisphere
93 (SH) atmospheric history of HFC-23 that was reasonably consistent with Oram et al., (1998)
94 results. Kim et al., (2010), reported HFC-23 measurements (November 2007-December 2008)
95 from Gosan, Jeju Island, South Korea and also estimated regional atmospheric emissions. Asian
96 emissions of HFC-23, including those for China have been reported by Yokouchi et al., 2006;
97 Stohl et al., 2010; Li et al., 2011; Yao et al., 2012. Most recently, Fang et al., (2014, 2015) have
98 provided bottom-up and top-down estimates of HFC-23 emissions from China and east Asia and
99 included observed HFC-23 mixing ratios at three stations - Gosan, South Korea, and Hateruma
100 and Cape Ochi-ishi, Japan. Remote sensing observations of HFC-23 in the upper troposphere
101 and lower stratosphere by two solar occultation instruments have also been reported (Harrison et
102 al., 2012), indicating an abundance growth rate of 5.8 ± 0.3% per year, similar to the CGAA
103 surface trend of 5.7 ± 0.4% per year over the same period (1989-2007).

104 HCFC-22 is used principally in air-conditioning and refrigeration, with minor uses in
105 foam blowing and as a chemical feedstock in the manufacture of fluoropolymers, such as
106 polytetrafluorethylene (PTFE). HCFC-22 production and consumption (excluding feedstock use)
107 are controlled under the Montreal Protocol. We have previously reported on the changing trends
108 and emissions of HCFC-22 (Simmonds et al., 2017 and references therein).

109 Technical solutions to mitigate HFC-23 emissions have included optimisation of the
110 HCFC-22 production process and voluntary and regulatory capture and incineration in
111 developed (Annex 1) countries (McCulloch, 2004). Mitigation in developing countries (Non-

Annex 1) has been introduced under the United Nations Framework Convention on Climate Change (UNFCCC) Clean Development Mechanism (CDM) to destroy HFC-23 from HCFC-22 production facilities (UNEP, 2017a). This allowed certain HCFC-22 production plants in developing countries to be eligible to provide Certified Emission Reduction (CER) credits for the destruction of the co-produced HFC-23. Beginning in 2003, there were 19 registered HFC-23 incineration projects in five developing countries with the number of projects in each country shown in parenthesis: China (11), India (5), Korea (1), Mexico (1) and Argentina (1) (Miller et al., 2010). The first CER credits under the CDM for HFC-23 abatement in HCFC-22 plants were approved in 2003 with funding through 2009. However, the CDM projects covered only about half of the HCFC-22 production in developing countries. The substantial reduction in global HFC-23 emissions during 2007-2009 was attributed by Miller et al. (2010) to the destruction of HFC-23 by CDM projects. In a subsequent paper, Miller and Kuijpers (2011) predicted future increases in HFC-23 emissions by considering three scenarios: a reference case with no additional abatement, and two opposing abatement measures, less mitigation and best practice involving increasing application of mitigation through HFC-23 incineration. Historically there has been a lack of information about HFC-23 emissions from the non-CDM HCFC-22 production plants, although Fang et al. (2015) provided a top-down estimate of HFC-23/HCFC-22 co-production ratios in non-CDM production plants. They reported that the HFC-23/HCFC-22 co-production ratios in all HCFC-22 production plants were 2.7% ± 0.4 by mass in 2007, consistent with values reported to the Executive Committee of the Montreal Protocol (UNEP, 2017a).

Here, we use the high frequency atmospheric observations of HFC-23 and HCFC-22 abundances measured by (GC-MS) at the five longest-running remote sites of the Advanced Global Atmospheric Gases Experiment (AGAGE). The site coordinates and measurement time frames of HFC-23 and HCFC-22 are listed in Table 1. To extend our understanding of the long-term growth rate of HFC-23, we combine the direct AGAGE atmospheric observations with results from an analysis of firn air collected in Antarctica and Greenland, a series of old Northern Hemisphere air samples, and archived air from the CGAA (Fraser et al. (1991). The AGAGE 2-D 12-box model and a Bayesian inversion technique are used to produce global emission estimates for HFC-23 and HCFC-22 (Cunnold et al., 1983; Rigby et al., 2011, 2014). We also include observations from the AGAGE Jungfraujoch station to determine estimates of European HFC-23 emissions (see section 3.3).

2. Methodology

2.1. AGAGE Instrumentation and Measurement Techniques

Ambient air measurements of HFC-23 and HCFC-22 at each site are made using the AGAGE GC-MS-Medusa instrument which employs an adsorbent-filled (HayeSep D) microtrap cooled to ~ -175°C to pre-concentrate the analytes during sample collection from 2 litres of air (Miller et al., 2008; Arnold et al., 2012). Samples are analysed approximately every 2 hours and are bracketed by measurements of quaternary standards to correct for short-term drifts in instrument response. Additional details of the analytical methodology are provided in the Supplementary material (1).

2.2. Firn and Archived Air

We used air samples from firn and archived in canisters to reconstruct an atmospheric HFC-23 history. Firn air samples from Antarctica and Greenland were analysed for HFC-23 using the same technology as the *in situ* measurements; details are provided in the Supplementary Material (2). The Antarctic samples were collected at the DSSW20K Law Dome site in 1997-1998 (Trudinger et al., 2002) and include one deep sample from the South Pole collected in 2001 (Butler et al., 2001). Greenland samples were collected at the NEEM (North Greenland Eemian Ice Drilling) site in 2008 (Buizert et al., 2012). The CSIRO firn model (Trudinger et al., 1997, 2013) was used to derive age spectra for the individual firn samples and more details on these samples and their analysis are given in Vollmer et al. (2016, 2018) and Trudinger et al. (2016). A diffusion coefficient of HFC-23 relative to CO_2 of 0.797 was used (Fuller et al., 1966).

CGAA measurements from three separate analysis periods were also used for the reconstruction of past HFC-23 abundances. The CGAA samples have been collected since 1978 at the Cape Grim Air Pollution Station and amount to >130 samples, the majority in internally electropolished stainless steel canisters (Fraser et al., 2016, 2017). Samples were analysed under varying conditions in 2006, 2011 and 2016. Here, we use a composite of the results from these measurement sets. Details are given in the Supplementary Material (2) and by Vollmer et al. (2018). A series of old Northern Hemisphere (NH) air samples were also measured together with the measurements of the CGAA samples at the Scripps Institution of Oceanography see Supplementary Material (2) and Mühle et al., (2010; Vollmer et al., (2016).

2.3. Calibration Scales

The estimated accuracies of the calibration scales for HFC-23 and HCFC-22 are discussed below and a more detailed discussion of the measurement techniques and calibration

procedures are reported elsewhere (Miller et al., 2008; O'Doherty et al., 2009; Mühle et al., 2010). HFC-23 and HCFC-22 measurements from all AGAGE sites are reported relative to the SIO-07 and SIO-05 primary calibration scales respectively, which are defined by suites of standard gases prepared by diluting gravimetrically prepared analyte mixtures in N_2O to near-ambient levels in synthetic air (Prinn et al., 2000; Miller et al., 2008).

The absolute accuracies of these primary standard scales are uncertain because possible systematic effects are difficult to quantify or even identify. Combining known statistical and estimated systematic uncertainties, such as measurement and propagation errors, and quoted reagent purities, generally yields lower uncertainties than are supported by comparisons among independent calibration scales (Hall et al., 2014). Furthermore, some systematic uncertainties may be normally distributed, while others, like reagent purity, are skewed in one direction. Estimates of calibration accuracies and their uncertainties are nevertheless needed for interpretive modelling applications. So, despite the difficulty in estimating unknown uncertainties, it is incumbent on those responsible for the measurements to provide an overall assessment of accuracy. Accordingly, we liberally estimate the absolute accuracies of these measurements as -3% to +2% for HFC-23 and ±1% for HCFC-22. The larger and asymmetric uncertainty for HFC-23 is due to its lower atmospheric and standard concentration, and to the lower stated purity of the HFC-23 reagent used to prepare the primary calibration scale.

2.4. Selection of baseline data (unpolluted background air)

Baseline *in situ* monthly mean HFC-23 and HCFC-22 mole fractions were calculated by excluding values enhanced by local and regional pollution influences, as identified by the iterative AGAGE pollution identification algorithm (for details, see Appendix in O'Doherty et al., 2001). Briefly, baseline measurements are assumed to have Gaussian distributions around the local baseline value, and an iterative process is used to filter out the data that do not conform to this distribution. A second-order polynomial is fitted to the subset of daily minima in any 121-day period to provide a first estimate of the baseline and seasonal cycle. After subtracting this polynomial from all the observations, a standard deviation and median are calculated for the residual values over the 121-day period. Values exceeding three standard deviations above the baseline are assigned as non-baseline (polluted) and removed from further consideration. The process is repeated iteratively to identify and remove additional non-baseline values until the new and previous calculated median values agree within 0.1%.

2.5. Bottom-up emissions estimates

The sources of information on production and emissions of HFCs are generally incomplete and do not provide a comprehensive database of global emissions. In Supplementary Material (3), we compile global HCFC-22 production and HFC-23 emissions data. HCFC-22 is used in two ways: (1) dispersive applications, such as refrigeration and air conditioning, whose production is controlled under the Montreal Protocol and reported by countries as part of their total HCFC production statistics, and (2) feedstock applications in which HCFC-22 is a reactant in chemical processes to produce other products. Although there is an obligation on countries to report HCFC-22 feedstock use to UNEP, this information is not made public. HCFC-22 production for dispersive uses was calculated from the UNEP HCFC database (UNEP, 2017b) and the Montreal Protocol Technology and Economic Assessment Panel 2006 Assessment (TEAP, 2006). Production for feedstock use was estimated using trade literature as described in the Supplementary Material (3) and the sum of production for dispersive and feedstock uses is shown in Table S3.

HFC-23 emissions from Annex 1 countries are reported as a requirement of the UNFCCC. Table S4 shows the total annual HFC-23 emissions reported by these countries (UNFCCC, 2017). There is a small uncertainty in these UNFCCC emissions due to whether countries report on a calendar or fiscal year basis. The data include emissions from use of HFC-23 in applications such as semi-conductor manufacture and fire suppression systems. These minor uses of HFC-23, originally produced in a HCFC-22 plant, will result in the eventual emission of most or all into the atmosphere and emissions have remained relatively constant at 0.13 ± 0.01 Gg yr^{-1}, a maximum of 10% of all emissions (UNFCCC, 2017). Non-Annex 1 countries listed in Table S4 were eligible for financial support for HFC-23 destruction under the CDM. Their emissions were calculated by applying factors to their estimated production of HCFC-22 and offsetting this by the amount destroyed under CDM, as described in the Supplementary Material (3). We discuss these independent emission estimates because they are useful as *a priori* data constraints ("bottom-up" emission estimates) which we compare to observation-based "top-down" estimates.

2.6. Global atmospheric model

Emissions were estimated using a Bayesian approach in which our *a priori* estimates of the emissions growth rate were adjusted by comparing modelled baseline mole fractions to the atmospheric observations (Rigby et al., 2011, 2014). The firn air measurements were included in the inversion, with the age spectra from the firn model used to relate the firn measurements to high-latitude atmospheric mole fractions (Trudinger et al., 2016; Vollmer et al., 2016). A 12-box

model of atmospheric transport and chemistry was used to simulate baseline mole fractions, which assumed that the atmosphere was divided into four zonal bands (90-30°N, 30-0°N, 0-30°S, 30-90°S) and at 500hPa and 200hPa vertically (Cunnold et al., 1994; Rigby et al., 2013). The model uses an annually repeating, monthly varying hydroxyl radical (OH) field from Spivakovsky et al (2000), which has been adjusted to match the observed trend in methyl chloroform (e.g. Rigby et al. 2013). For the gases in this paper, potential variations in OH concentration (e.g. Rigby et al., 2017) were not found to lead to a large change in the derived emissions (see Supplementary Material 4). Annually repeating, monthly varying transport parameters were used as described in Rigby et al., (2014). The temperature-dependent rate constant for reaction with OH was taken from Burkholder et al. (2015), which led to a lifetime of 237 yr for HFC-23 and 11.6 yr for HCFC-22. As in previous publications (e.g. Rigby et al., 2014), uncertainties in the monthly mean baseline observations in each semi-hemisphere were taken to be the quadratic sum of the measurement repeatability and the variability of the observations within the month that were flagged as "baseline", using the method in O'Doherty et al. (2001). The variability was used to approximate model uncertainty, as it was assumed to be a measure of the time scales not resolved by the model. No correlated uncertainties were assumed in the model-measurement mismatch uncertainty and both the model-measurement mismatch and the *a priori* constraint were assumed to be described by Gaussian probability density functions. Seasonal emissions estimates in each semi-hemisphere were derived in the inversion. The inversion propagates uncertainty estimates from the measurements, model and prior emissions growth rate to these *a posteriori* emissions estimates. The prior emissions growth rate uncertainty was somewhat arbitrarily chosen at a level of 20% of the maximum *a priori* emissions and no correlation was assumed between prior estimates of annual emissions growth rate. In contrast to Rigby et al. (2014), in which a scaling factor of the emissions was solved for in the inversion, here we determined absolute emissions, which were found to lead to more robust uncertainty estimates when emissions were very low. *A posteriori* emissions uncertainties were augmented with an estimate of the influence of uncertainties in the lifetime, as described in Rigby et al. (2014).

2.7. Regional scale atmospheric inversion

HFC-23 pollution events are still observed at sites in north east Asia and Europe. The former have recently been used in regional scale inverse modelling studies to derive emission estimates for the Asian region and these results are summarised in Section 3.3. In contrast, little attention has recently been given to HFC-23 emissions from Europe. We examine European emissions, using a regional scale inversion tool based on source sensitivities as estimated by a Lagrangian Particle Dispersion Model run in backward mode, combined with a Bayesian inversion framework.

2.7.1. Transport simulations

Surface source sensitivities were computed with the Lagrangian Particle Dispersion Model (LPDM) FLEXPART (Stohl et al., 2005) driven by operational analysis/forecasts from the European Centre for Medium-Range Weather Forecasts (ECMWF) Integrated Forecasting System (IFS) modelling system with a horizontal resolution of 0.2° x 0.2° for central Europe and 1° x 1° elsewhere. 50,000 model particles were released for each 3-hourly time interval and followed backward in time for 10 days.

2.7.2. Bayesian inversion framework

A spatially resolved, regional-scale emission inversion, using the FLEXPART-derived source sensitivities and a Bayesian approach was applied to estimate European HFC-23 annual emissions for individual years between 2009 and 2016. The details of the inversion method were recently published in estimating Swiss methane emissions (Henne et al., 2016). This inversion methodology was part of an HFC inversion inter-comparison (Brunner et al, 2017) and was applied to HFC and HCFC emissions in the eastern Mediterranean (Schönenberger et al., 2017). Here, the inversion relies on the continuous observations from the Jungfraujoch and Mace Head and requires *a priori* estimates of the emissions distribution. The observations are split into a baseline concentration and above-baseline excursions of the signal that are attributed to recent emissions using the method of Ruckstuhl et al. (2012). The inversion estimates spatially distributed, annual mean emissions and a two-weekly concentration baseline. In the case of HFC-23 the baseline concentration is very well defined due to the relatively infrequent occurrence of larger pollution events. The inversion results were not significantly different when the baseline was not updated as part of the inversion. The spatial distribution was solved on a grid with different sized rectangular cells. The grid size was inversely proportional to annual total source sensitivities and, therefore, was finer close to the measurement sites and coarser in more remote regions that seldom influence the sites. In contrast to previous applications, the grid resolution was also increased around likely point emitters in order to better localise these potentially large contributors.

In this study the inversion was set up using complete covariance matrices. We designed the *a priori* covariance matrix in such a way that the total *a priori* uncertainty for each of the regions/countries was 200% and proportional to the emissions in each inversion grid cell. Off-diagonal elements of the matrix were filled with the assumption of exponentially decaying spatial correlation of the uncertainties with a length scale of 10 km. The choice of this rather

small spatial correlation scale was motivated by the assumed strong contribution from point source emissions, which should result in spatially rather uncorrelated *a priori* uncertainties. The data-mismatch covariance matrix contained uncertainty elements that describe the uncertainty of the observations and the transport model. The observation uncertainty was taken from target gas measurements, whereas the model uncertainty was estimated as the RMSE (root mean square) of the *a priori* simulations Henne et al., (2016). The off-diagonal elements of the covariance matrix were again assumed to exponentially decay with time between the data points. The resulting correlation time scale was estimated separately for each site from a fit to the auto-correlation function of the prior model residuals (see Schönenberger et al., 2017) and was in the order of 0.2 to 0.3 days.

2.7.3. *A priori* emissions and sensitivity inversions

Spatially distributed *a priori* emissions were generated from individual national inventory reports (NIR) to UNFCCC (2017). Most European countries separately list the emissions of HFC-23 by sector in Table 2(II) of their submissions. Here, we chose two different approaches to spatially distribute these bottom-up estimates and use these as input for two sensitivity inversions. In the first approach (UNFCCC_org), we directly follow the categorisation in each NIR and assign emissions from 'Fluorochemical production' to individual production sites as taken from Keller et al. (2011), and shown in Figure S4, whereas emissions from 'Electronics industry' and 'Product use' were distributed according to population density (Center for International Earth Science Information Network - CIESIN - Columbia University. 2016, available at https://ciesin.columbia.edu/data/hrsl/). Countries reporting no or zero HFC-23 emissions were assigned a *per capita* emission factor equal to 1/10 of the average *per capita* emission factor from reporting countries. This mostly impacts countries at the periphery of the inversion domain. In our second approach (UNFCCC_r0.5), we used the same spatial disaggregation as before, but assigning 50% of the 'Electronics industry' and 'Product use' emissions in each country to the likely point source locations and distribute the remainder by population. Inversions using the HFC-23 inventory provided by EDGAR (version 4.2) as *a priori* were tested. However, these inversions showed much weaker model performance than those based on UNFCCC priors and, hence, were dropped from any further analysis.

3. Results and Discussion

3.1. Atmospheric mole fractions

Figure 1 shows the HFC-23 modelled mole fraction for the four equal-mass latitudinal subdivisions of the global atmosphere calculated from the 12-box model and the combined GC-MS-Medusa *in situ* measurements (2008-2016), firn air data, old NH air and CGAA data. The lower box shows the annual growth rates in pmol mol^{-1} yr^{-1}. We find that the global modelled annual mole fraction of HFC-23 in the background atmosphere reached 28.9 ± 0.6 pmol mol^{-1}, (1σ confidence interval) in December 2016, a 163% increase from 1995 and a 28% increase from the 22.6 ±0.2 pmol mol^{-1} reported in 2009 (Miller et al., 2010). In 2008 the annual mean mid-year growth rate of HFC-23 was 0.78 pmol mol^{-1} yr^{-1}. By mid-2009 the growth rate decreased to 0.68 pmol $mol^{-1}yr^{-1}$, rising to a maximum of 1.05 pmol mol^{-1} yr^{-1} in early 2014, followed by a smaller decrease to 0.95 pmol mol^{-1} yr^{-1} in 2016. The growth rate of HFC-23 increased by 22 % from 2008 to 2016. In the Figure 1 inset, we compare the annual mean mole fractions of HFC-23 and HCFC-22 recorded at Mace Head and Cape Grim, as examples of mid-latitude northern hemisphere (NH) and southern hemisphere (SH) sites, illustrating the site divergence for these two compounds beginning around 2010.

Figure 2 shows our HCFC-22 modelled mole fractions for the four equal-mass latitudinal subdivisions of the global atmosphere calculated from the 12-box model and the lower box shows the HCFC-22 annual growth rates in pmol mol^{-1} yr^{-1}. The global modelled HCFC-22 annual mixing ratio in the background atmosphere reached peaked at 238 ± 2 pmol mol^{-1} in December 2016, following the decline in the annual average global growth rate of HCFC-22 from 2008 to 2016 of 0.5 pmol mol^{-1} yr^{-2}. This decline in the global growth rate of HCFC-22 coincides with the phase out of HCFC production/consumption mandated by the 2007 amendment to the Montreal Protocol for Annex 1 countries, covering dispersive applications, but not the non-dispersive use of HCFC-22 as a feedstock in fluoropolymer manufacture (UNEP, 2017a). Nevertheless, HCFC-22 remains the dominant HCFC in the atmosphere and accounts for 79% by mass of the total global HCFC emissions (Simmonds et al., 2017). In contrast to the increasing growth rate of HFC-23, the growth rate of HCFC-22 has exhibited a steep 53% decline from a maximum in January 2008 of 8.2 pmol $mol^{-1}yr^{-1}$ to 3.8 pmol mol^{-1} yr^{-1} in December 2016, further illustrating the divergence between these two gases between 2008 and 2016 (compare lower boxes in Figures 1 and 2). These results are an update of our previously reported analysis AGAGE HCFC-22 data (Simmonds et al., 2017) for the period 1995-2015.

3.2. Global emission estimates

Miller et al. (2010) calculated global emissions of HFC-23 using the same AGAGE 12-box model as used here, but with a different Bayesian inverse modelling framework. Following a peak in emissions in 2006 of 15.9 (+1.3/-1.2) Gg yr^{-1}, modelled emission estimates of HFC-23 declined rapidly to 8.6 (+0.9/-1.0) Gg yr^{-1} in 2009, which Miller noted was the lowest annual emission for the previous 15 years. Based on the analysis of firn air samples and ambient air measurements from Antarctica, Montzka et al. (2010) reported global HFC-23 emissions of 13.5 ± 2 Gg yr^{-1} (200 ± 30 Mt CO_2-e yr^{-1}), averaged over 2006-2008. In Carpenter and Reimann (2014), global emissions of HFC-23 estimated from measured and derived atmospheric trends reached a maximum of 15 Gg yr^{-1} in 2006, declined to 8.6 Gg in 2009, and subsequently increased again to 12.8 Gg in 2012 (Figure 1-25, update of Miller et al., 2010 and Montzka et al., 2010).

The model derived HFC-23 emissions from this study, shown in Figure 3 and listed in Table 2, reached an initial maximum in 2006 of 13.3 ± 0.8 Gg yr^{-1}, then declined steeply to 9.6 ± 0.6 Gg yr^{-1} in 2009. Our HFC-23 emissions estimates, which include firn data and NH archive air samples and a slightly different inverse method, are slightly lower in 2006 and slightly higher in 2009 than the HFC-23 estimates of Miller et al. (2010) and Carpenter and Reimann (2014) respectively. Our mean annual (2006-2008) HFC-23 emissions of 12.1 (± 0.7) Gg yr^{-1} are lower than the Montzka et al., (2010) emissions estimates of 13.5 ± 2 Gg yr^{-1}, but agree within uncertainties. However, our HFC-23 emissions then grew rapidly reaching a new maximum of 14.5 ± 0.6 Gg yr^{-1} (180 ± 7 Mt CO_2-eq yr^{-1}) in 2014, only to decline again to 12.7 ± 0.6 Gg yr^{-1} (157 ± 7 Mt CO_2-eq yr^{-1}) in 2016. Cumulative HFC-23 emissions estimates from 2010 to 2016 were 89 ± 16 Gg (1.1 ± 0.2 Gt CO_2-e), contributing to an increase in radiative forcing of 1.0 ± 0.1 mW m^{-2}.

The global emission estimates for HCFC-22 are plotted in Figure 4 together with the corresponding Miller et al. (2010) emissions up to 2008 and the WMO 2014 emissions estimates (Carpenter and Reimann, 2014). Table 3 lists the global emission estimates, mole fractions and growth rate of HCFC-22. Our modelled HCFC-22 emissions reached a maximum global maximum of 385 ± 41 Gg yr^{-1} (696 ± 74 Mt CO_2-eq yr^{-1}) in 2010, followed by a slight decline to 370 ± 46 Gg yr^{-1} (670 ± 83 Mt CO_2-eq yr^{-1}) in 2016 at an annual average rate of 2.3 Gg yr^{-1}.

3.3. Regional emissions

Several papers report Asian emissions of HFC-23, including those for China (Yokouchi et al., 2006; Stohl et al., 2010; Kim et al., 2010; Li et al., 2011; Yao et al., 2012). Recent papers by Fang et al. (2014, 2015) noted inconsistencies between the various bottom-up and top-down

emissions estimates and provided an improved bottom-up inventory and a multi-annual top-down estimate of HFC-23 emissions for east Asia. They showed that China contributed 94-98 % of all HFC-23 emissions in east Asia and was the dominant contributor to global emissions: 20 ± 6 % in 2000 rising to 77 ± 23 % in 2005. China's annual HFC-23 top-down emissions in 2012 were estimated at 8.8 ± 0.8 Gg yr^{-1} (Fang et al., 2015), 69% of our 2012 global emissions estimate of 12.9 ± 0.6 Gg yr^{-1}, listed in Table 2.

Based on the bottom-up estimated global HFC-23 emissions (shown in Supplementary Material (3), Table S4), we show in Figure 5a global and Chinese emissions and the percentage of Chinese emissions contributing to the global total. These bottom-up estimates show that a steadily increasing fraction of global total HFC-23 emissions can be attributed to China, averaging about 88% in 2011-2014. This rise is consistent with the increase in our calculated bottom-up HCFC-22 production data compiled from industry sources and listed in Supplementary Material (3), Table S3. Figure 5b, shows the bottom-up estimates of global and China HCFC-22 production and the percentage contribution of China production to the global total, further illustrating the dominance of HCFC-22 production in China.

Clearly China is the major contributor to recent global HFC-23 emissions which implies only minor contributions from other regional emitters. However, HFC-23 pollution events are still observed at our European sites. Keller et al. (2011) reported European HFC-23 emissions based on inverse modelling for the period summer 2008 to summer 2010, assigning most of the emissions to point sources at HCFC-22 production sites. Here, we re-evaluated European HFC-23 emissions for the period 2009 to 2016 (see section 2.7). The key results from this analysis are summarised in Figures 6 and in Table 4 and more detailed results are available in the Supplementary Material (5).

Based on these inversion results, European emissions of HFC-23, though small on a global scale were, in general, larger than reported to UNFCCC and exhibited considerable year-to-year variability (Table 4, Figure 6 and spatial distribution Figure S4). Total *a posteriori* emissions for the six European regions reached a maximum of 0.30 ± 0.05 Gg yr^{-1} in 2013 declining to 0.17 ± 0.03 Gg yr^{-1} in 2016 and showed a slightly negative, statistically insignificant trend over the period analysed (2009-2016). The cumulative European HFC-23 emissions from 2010-2016 were ~1.3 Gg corresponding to just 1.5% of our cumulative global HFC-23 emissions over this same period of 89 Gg (Table 2). Considerable differences between the two inversions with different *a priori* emission distributions (see section 2.7.3) were observed on a country scale, with generally larger Italian *a posteriori* emissions when the original UNFCCC split of point and area sources was used in the *a priori* (UNFCCC_org). In this case the inversion

was not able to completely relocate the area emissions, but at the same time increased emissions at the point source locations and resulting in overall larger *a posteriori* emissions. For both sensitivity inversions the fraction of European emissions within grid boxes containing HCFC-22 production facilities, increased in the *a posteriori* as compared with the *a priori* distribution (Table 4 and Figure S4).

In the following section we attempt to reconcile the changing trends in global HFC-23 emissions with the decrease in global HCFC-22 emissions after 2010 and the decline in the annual HCFC-22 growth rate. There are a number of key factors which we believe can explain the changing trend in the recent history of HFC-23 emissions after the minimum in 2009.

3.4. Factors affecting the recent increase in HFC-23 emissions and changes in the consumption of produced HCFC-22.

1. Recent publications have highlighted the substantial increase in HCFC-22 production in Non-Annex 1 countries since the 1990s, especially in the last decade, due to increasing demand in air-conditioning, refrigeration applications and primarily from the use of HCFC-22 as a feedstock in fluoropolymer manufacture (UNEP, 2009; Miller et al., 2010; USEPA, 2013; Fang et al., 2015). This has resulted in Non-Annex 1 countries emitting more co-produced HFC-23 than Annex 1 countries since about 2001 (Miller et al., 2010). HCFC-22 production in Annex 1 countries in 2015 had shrunk by 45% from the peak historic value of 407 Gg yr^{-1} in 1996 (see Supplementary Material (3), Table S3). This has been accomplished by plant closures and further reductions of HFC-23 emissions by enhanced destruction in the remaining plants. Nevertheless, ~ 1 Gg of HFC-23 was emitted in 2015 from HCFC-22 production in Annex 1 countries, mainly from Russia and USA (96%). For comparison, the combined HFC-23 emissions in 2015 from the six European regions (listed in Table 4) were just 0.11 ± 0.03 Gg.

2. Since 2006, a major factor mitigating HFC-23 emissions has been the CERs issued under the CDM. However, under the original CDM rules, large CERs that cost relatively little to acquire could be claimed legitimately (Munnings et al., 2016) and the rules were changed to bar new entrants to the mechanism after 2009. The HFC-23/HCFC-22 co-production or waste gas generation ratio varies between 1.5 - 4% (by mass) depending on HCFC-22 plant operating conditions and process optimization (McCulloch and Lindley, 2007). Under the UNFCCC/CDM, 19 HCFC-22 production plants in five Non-Annex 1 countries - Argentina (1), China (11), Democratic People's Republic of Korea (1), India (5) and Mexico (1) - were approved for participation in CDM projects. These countries reportedly incinerated 5.7 Gg and 6.8 Gg of HFC-23 in 2007 and 2008, respectively (UNFCCC, 2009). This represented 43 - 48%

of the HCFC-22 produced in Non-Annex 1 countries during 2007-2008 assuming the 1.5 - 4% co-production factor (Montzka et al., 2010). These five countries produced 597 Gg of HCFC-22 from controlled and feed stock uses in 2015. HFC-23 generated from this HCFC-22 production was estimated at 16 Gg with an average co-production ratio of 2.6%. Furthermore, it was estimated that China produced 535 Gg of HCFC-22 in 2015 (~90% of the five countries' total production) and 45% of the co-produced HFC-23 generated was destroyed in the CDM destruction facilities (UNEP, 2017a). The first seven-year crediting period of CDM projects in China expired in 2013, concurrent with the European Union ceasing the purchase of CER credits for HFC-23 produced in industrial processes after May 2013 (Fang et al., 2014).

3. Lastly, we should consider whether there are other sources of HFC-23 which might explain an increase in global emissions. While the major source of all HFC-23 is HCFC-22 co-production, material that is recovered and sold may subsequently be emitted to the atmosphere. Emissions of HFC-23 from fire suppression systems are negligible relative to global production (McCulloch and Lindley, 2007) and emissions from all emissive uses are reported to be 0.13 ± 0.01 Gg yr^{-1} from Annex 1 countries (UNFCCC, 2017) and less than 0.003 Gg for the refrigeration and fire-fighting sectors in 2015 in the five Non-Annex 1 countries listed above, (UNEP, 2017a). Semi-conductor use of HFC-23 is insignificant having been replaced by more efficient etchants and where destruction efficiencies are greater than 90% (Bartos et al., 2006, Miller et al., 2010). Fraser et al. (2013) reported a very small emissions factor of 0.04 g HFC-23 Mg^{-1} aluminium (Al) from the Kurri Kurri smelter in NSW, Australia. It was estimated that this corresponds to an annual emission of HFC-23 from Al production of ~0.003 Gg based on a global Al production of 57 Tg in 2016 (http://www.world-aluminium.org/statistics/#data, accessed 2016). Realistically, these other potential industrial sources of HFC-23 emissions are very small (< 0.015 Gg yr^{-1}) in the context of global emissions estimates.

The combination of these factors strongly suggests that the steep reversal of the downwards trend in HFC-23 emissions after 2009 is attributable to HFC-23 abatement measures not being adequate to offset the increasing growth in production of HCFC-22 for non-dispersive feedstock. This is despite the initial success of CDM abatement technologies leading to mitigation of HFC-23 emissions during 2006-2009.

4. Conclusions

The introduction of CERs under the CDM did contribute to a reduction of HFC-23 emissions in Non-Annex 1 countries during 2006-2009, thereby lowering global emissions, reaching a minimum of 9.6 ± 0.6 Gg yr^{-1} in 2009. However, from 2010 to 2014 global HFC-23

519 emissions increased steadily at an annual average rate of ~1 Gg yr^{-1} reaching a new maximum of
520 14.5 ± 0.6 Gg yr^{-1} in 2014. This period coincides with the highest levels of our bottom-up
521 estimates of HCFC-22 production in Non-Annex 1 countries (Supplementary Material (3), Table
522 S3), coinciding with a transition period when HCFC-22 production plants without any abatement
523 controls had yet to install incineration technologies or fully adopt process optimisation
524 techniques. Furthermore, non-CDM plants are not required to report co-produced HFC-23
525 emissions, although Fang et al. (2015) calculated that these plants have a lower HFC-23/HCFC-
526 22 production ratio as they came into operation after the CDM period and would most likely be
527 using improved technologies for HFC-23 abatement.
528 Our cumulative HFC-23 emissions estimates from 2010 to 2016 were 89.1 ± 4.3 Gg (1.1 ± 0.2
529 Gt CO_2-eq), which led to an increase in radiative forcing of 1.0 ± 0.1 mW m^{-2}. This implies that
530 the post-2009 increase in HFC-23 emissions resulted from the decision not to award new CDM
531 projects after 2009, against a background of increasing production of HCFC-22 in plants that did
532 not have abatement technology. Over this same time frame, the magnitude of the cumulative
533 emissions of HCFC-22 was 2610 ± 311 Gg (4724 Mt CO_2-eq yr^{-1}). During 2015-2016 our results
534 show a decline of about 9% in average global HFC-23 emissions (12.9 Gg yr^{-1}) relative to the
535 2013-2014 average of 14.2 Gg yr^{-1}. We note that in the Kigali 2016 Amendment to the Montreal
536 Protocol, China committed to a domestic dispersive HCFC-22 production reduction of 10% by
537 2015 compared to the average 2009-2010 production (UNEP, 2017a). While this regulation
538 should decrease HCFC-22 production for dispersive uses, overall HFC-23 emissions could still
539 continue to increase due to a potential increase in the production of HCFC-22 for feedstock uses
540 (Fang et al., 2014). It is perhaps encouraging that the Kigali Amendment also stipulates that the
541 Parties to the Montreal Protocol shall ensure that HFC-23 emissions generated from production
542 facilities producing HCFCs or HFCs are destroyed to the maximum extent possible using
543 technology yet to be approved by the Parties. In 2014, with the support of the Chinese
544 Government, 13 new destruction facilities at 15 HCFC-22 production lines not covered by
545 CDM, were installed (UNEP, 2017a). The time frame of these new initiatives is consistent with
546 the most recent reduction (2015-2016) of global HFC-23 emissions.
547 The mismatch between mitigation and emissions, that is most evident in China, suggests
548 that the delay in the implementation of additional abatement measures allowed HFC-23
549 emissions to increase before these measures became effective. Our results imply that HFC-23
550 emissions into the atmosphere will continue to increase and make a contribution to radiative
551 forcing of HFCs until the implementation of abatement becomes a universal requirement.
552
553

Acknowledgements

We specifically acknowledge the cooperation and efforts of the station operators (G. Spain, Mace Head, Ireland; R. Dickau, Trinidad Head, California; P. Sealy, Ragged Point, Barbados; NOAA Officer-in-Charge, Cape Matatula, American Samoa; S. Cleland, Cape Grim, Tasmania) and their staff at all the AGAGE stations. The operation of the AGAGE stations was supported by the National Aeronautics and Space Administration (NASA, USA) (grants NAG5-12669, NNX07AE89G, NNX11AF17G and NNX16AC98G to MIT; grants NAG5-4023, NNX07AE87G, NNX07AF09G, NNX11AF15G, NNX11AF16G, NNX16AC96G and NNX16A97G to SIO). We acknowledge the Department for Business, Energy and Industrial Strategy (BEIS, UK) for contract 1028/06/2015 to the University of Bristol and the UK Meteorological Office in support of Mace Head, Ireland, and modelling activities; the National Oceanic and Atmospheric Administration (NOAA, USA), contract RA-133-R15-CN-0008 to the University of Bristol in support of Ragged Point, Barbados; we acknowledge NOAA support for the operations of the American Samoa station, and support by the Commonwealth Scientific and Industrial Research Organisation (CSIRO, Australia), the Bureau of Meteorology (Australia) and Refrigerant Reclaim Australia for Cape Grim operations.

CSIRO's contribution was supported in part by the Australian Climate Change Science Program (ACCSP), an Australian Government Initiative. Australian firn activities in the Antarctic are specifically supported by the Australian Antarctic Science Program. We acknowledge the members of the firn air sampling teams for provision of the samples from Law Dome, NEEM, and South Pole. NEEM is directed and organized by the Centre of Ice and Climate at the Niels Bohr Institute and US NSF, Office of Polar Programs. It is supported by funding agencies and institutions in Belgium (FNRS-CFB and FWO), Canada (NRCan/GSC), China (CAS), Denmark (FIST), France (IPEV, CNRS/INSU, CEA, and ANR), Germany (AWI), Iceland (RannIs), Japan (NIPR), Korea (KOPRI), the Netherlands (NWO/ALW), Sweden (VR), Switzerland (SNF), United Kingdom (NERC), and the U.S. (U.S. NSF, Office of Polar Programs). Financial support for the Jungfraujoch measurements is acknowledged from the Swiss national programme HALCLIM (Swiss Federal Office for the Environment (FOEN)). Support for the Jungfraujoch station was provided by International Foundation High Altitude Research Stations Jungfraujoch and Gornergrat (HFSJG).

M. Rigby is supported by a NERC Advanced Fellowship NE/I021365/1. We acknowledge the cooperation of R. Langenfelds for his long-term involvement in supporting and maintaining the Cape Grim Air Archive. We also thank S. Montzka and B. Hall for supplying actual datasets from their publications.

589 **References.**

590 Arnold, T., Mühle, J., Salameh, P. K., Harth, C.M., Ivy, D. J., and Weiss, R. F.: Automated
591 measurement of nitrogen trifluoride in ambient air, Anal. Chem., 84, 4798–4804, 2012.

592 Bartos, S., Beu, L. S., Burton, C. S., Fraust, C. L., Illuzzi, F., Mocella, M. T., and Raoux, S.:
593 IPCC Guidelines for National Greenhouse Inventories. Volume 3, Industrial Processes, Chapter
594 6, Electronics Industry, available at: www.ipcc-nggip.iges.or.jp/public/2006gl/pdf/3.
595 Volume3/V3.6.Ch6_Electronics .Industry, pdf, 2006.

596 Brunner, D., Arnold, T., Henne, S., Manning, A., Thompson, R. L., Maione, M., O'Doherty, S.,
597 and Reimann, S.: Comparison of four inverse modelling systems applied to the estimation of
598 HFC-125, HFC-134a and SF_6 emissions over Europe, Atmos. Chem. Phys., 17, 10651-10674,
599 https://doi.org/10.5194/acp-17-10674-2017, 2017.

600 Burkholder, J. B., Sander, S. P., Abbatt, J., Barker, R., Huie, R. E., Kolb, C. E., Kurylo, M. J.,
601 Orkin, V. L., Wilmouth, D. M., and Wine, P.H.: Chemical kinetics and photochemical data for
602 use in atmospheric studies, Evaluation No. 18, JPL Publication 15-10, Jet Propul. Lab.,
603 Pasadena, Calif, 2015. [available at http://jpldataeval.jpl.nasa.gov.]

604 Buizert, C., Martinerie, P., Petrenko, V. V., Severinghaus, J. P., Trudinger, C. M., Witrant, E.,
605 Rosen, J. L., Orsi, A. J., Rubino, M., Etheridge, D. M., Steele, L. P., Hogan, C., Laube, J. C.,
606 Sturges, W. T., Levchenko, V. A., Smith, A. M., Levin, I., Conway, T. J., Dlugokencky, E. J.,
607 Lang, P. M., Kawamura, K., Jenk, T. M., White, J. W. C., Sowers, T., Schwander, J., and
608 Blunier, T.: Gas transport in firn: multiple-tracer characterisation and model intercomparison for
609 NEEM, Northern Greenland, Atmos. Chem. Phys., 12, 4259–4277, doi:10.5194/acp-12-4259-
610 2012.

611 Butler, J. H., Montzka, S. A., Battle, M., Clarke, A. D., Mondeel, D. J., Lind, J. A., Hall, B. D.,
612 and Elkins, J. W.: Collection and analysis of firn air from the South Pole, 2001, AGU Fall
613 Meeting Abstracts, p. F145, 2001.

614 Carpenter, L. J. and Reimann, S.: Ozone-Depleting Substances (ODSs) and Other Gases of
615 Interest to the Montreal Protocol, Chapter 1, in: Scientific Assessment of Ozone Depletion:
616 2014, Global Ozone Research and Monitoring Project - Report No. 55, World Meteorological
617 Organisation, Geneva, Switzerland, 2014.

618 Culberston, J. A., Prins, J. M., Grimsrud, E. P., Rasmussen, R.A., Khalil, M. A. K., and Shearer,
619 M. J.: Observed trends in CF_3-containing compounds in background air at Cape Meares,
620 Oregon, Point Barrow, Alaska, and Palmer Station, Antarctica, Chemosphere, 55, 1109–1119,
621 2004.
622
623 Cunnold, D. M., Prinn, R.G., Rasmussen, R., Simmonds, P. G., Alyea, F. N., Cardlino, C.,
624 Crawford, A. J., Fraser, P. J., Rosen, R.: The Atmospheric Lifetime Experiment, III: lifetime
625 methodology and application to three years of $CFCl_3$ data, J. Geophys. Res., 88, 8379-8400,
626 1983.

627 Cunnold, D. M., Fraser, P. J., Weiss, R. F., Prinn, R. G., Simmonds, P. G., Miller, B. R., Alyea,
628 F. N., Crawford, A. J., and Rosen, R.: Global trends and annual releases of CCl_3F and CCl_2F_2

estimated from ALE/GAGE and other measurements from July 1978 to June 1991, J. Geophys. Res., 99, 1107-1126, 1994.

Fang, X., Miller, B. R., Su, S., Wu, J., Zhang, J., and Hu, J.: Historical emissions of HFC-23 (CHF_3) in China and projections upon policy options by 2050, Environ. Sci. & Technol, 48, 4056-4062, 2014.

Fang, X., Stohl, A.,Yokouchi, Y., Kim, J., Li, S., Saito, T., Park S and Hu. J.: Multiannual top-down estimate of HFC-23 emissions in east Asia. Environ. Sci. & Technol, 49, 4345-4353, 2015.

Fraser, P. J., Langenfelds, R.L., Derek N and Porter, L.W.: Studies in air archiving techniques, in Baseline Atmospheric Program (Australia) 1989, S. R. Wilson and J. L. Gras (eds.), Department of the Arts, Sport, the Environment, Tourism and Territories, Bureau of Meteorology and CSIRO Division of Atmospheric Research, Canberra, Australia, 16-29, 1991.

Fraser, P., Steele, L.P., and Cooksey, M.: PFC and carbon dioxide emissions from an Australian aluminium smelter using time-integrated stack sampling and GC-MS, GC-FID analysis. Light Metals 2013, B. Sadler (ed.), Wiley/TMS 2013, 871-876, 2013.

Fraser, P. J., Steele, L.P., Pearman, G.I., Coram, S., Derek, N., Langenfelds, R.L and Krummel, P.B.: Non-carbon dioxide greenhouse gases at Cape Grim: a 40 year odyssey, Baseline Atmospheric Program (Australia) History and Recollections, 40th Anniversary Special Edition, Derek, N., P. B. Krummel and S. J. Cleland (eds.), Bureau of Meteorology/CSIRO Oceans and Atmosphere, ISSN 0155-6959, 45-76, 2016.

Fraser, P. J., Pearman, G and Derek, N., I. CSIRO non-carbon dioxide greenhouse gas research. Part 1: 1975-1990, Historical Records of Australian Science, doi.10.1071/HR17016, 2017.

Fuller, E. N., Schettler, P. D., and Giddings, J. C.: A new method for prediction of binary gas-phase diffusion coefficients, Ind. Eng. Chem., 30, 19–27, 1966.

Hall, B.D., Engel, A., Mühle, J., Elkins, J. W., Artuso, F., Atlas, E., Aydin, M., Blake, D., Brunke, E.-G., Chiavarini, S., Fraser, P. J., Happell, J., Krummel, P. B., Levin, I., Loewenstein, M., Maione, M., Montzka, S. A., O'Doherty, S., Reimann, S., Rhoderick, G., Saltzman, E. S., Scheel, H. E., Steele, L. P., Vollmer, M. K., Weiss, R. F., Worthy, D., and Yokouchi, Y. 2014., Results from the International Halocarbons in Air Comparison Experiment (IHALACE), Atmos. Meas. Tech, 72, 469-490, doi:10.5194/amt-7-469-2014, 2014.

Harrison, J. J., Boone, C. D., Brown, A. T., Allen, N. D. C., Toon, G. C., and Bernath, P. F.: First remote sensing observations of trifluoromethane (HFC-23) in the upper troposphere and lower stratosphere, J. Geophys. Res., 117, D05308, doi: 10.1029/2011JD016423, 2012.

Henne, S., Brunner, D., Oney, B., Leuenberger, M., Eugster, W., Bamberger, I., Meinhardt, F., Steinbacher, M., and Emmenegger, L.: Validation of the Swiss methane emission inventory by atmospheric observations and inverse modelling, Atmos. Chem. Phys., 16, 3683-3710, doi: 10.5194/acp-16-3683-2016, 2016.

Keller, C. A., Brunner, D., Henne, S., Vollmer, M. K., O'Doherty, S., and Reimann, S.: Evidence for under-reported western European emissions of the potent greenhouse gas HFC-23. Geophys. Res. Lett, 38, L15808, doi: 10.1029/2011GL047976, 2011.

Kim, J., Li, S., Kim, K. R., Stohl, A., Mühle, J., Kim, S. K., Park, M. K., Kang, D. J., Lee, G., Harth, C. M., Salameh, P. K., and Weiss, R. F.: Regional atmospheric emissions determined from measurements at Jeju Island, South Korea: halogenated compounds from China, Geophys. Res. Lett, 37, doi:10.1029/2010GL043263, 2010.

Li, S.; Kim, J.; Kim, K. R.; Mühle, J.; Kim, S. K.; Park, M. K.; Stohl, A.; Kang, D. J.; Arnold, T.; Harth, C. M.; Salameh, P. K.; Weiss, R. F.: Emissions of halogenated compounds in East Asia determined from measurements at Jeju Island, Korea, Environ. Sci. Technol., 45 (13), 5668−5675, 2011.

McCulloch, A.: Incineration of HFC-23 Waste Streams for Abatement of Emissions from HCFC-22 Production: A Review of Scientific, Technical and Economic Aspects, commissioned by the UNFCCC secretariat to facilitate the work of the Methodologies Panel of the CDM Executive Board, available online at: http: //cdm.unfccc.int/methodologies/Background 240305.pdf, 2004.

McCulloch, A., and Lindley, A. A.: Global Emissions of HFC-23 estimated to year 2015. Atmos. Environ, 41, 1560-1566, 2007.

Miller, B, R., Weiss, R. F., Salameh, P. K., Tanhua, T., Greally. B, R., Mühle, J., Simmonds, P, G.: Medusa: A sample pre-concentration and GC-MS detector system for *in situ* measurements of atmospheric trace halocarbons, hydrocarbons and sulphur compounds, Anal. Chem., 80, 1536-1545, 2008.

Miller, B. R., Rigby, M., Kuijpers, L. J. M., Krummel, P. B., Steele, L. P., Leist, M., Fraser, P. J., McCulloch, A., Harth, C. M., Salameh, P.K., Mühle, J., Weiss, R. F., Prinn, R.G., Wang, R. H. J., O'Doherty, S., Greally, B. R., and Simmonds, P. G.: HFC-23 (CHF_3) emission trend response to HCFC-22 ($CHClF_2$) production and recent HFC-23 emissions abatement measures, Atmos. Chem. Phys, 10, 7875-7890, 2010.

Miller, B. R., and Kuijpers, L. J. M.: Projecting future HFC-23 emissions, Atmos. Chem. Phys., 11, 13259-13267, doi:10.5194/acp-11-13259-2011, 2011

Miller, M., and Batchelor, T.: Information paper on feedstock uses of ozone-depleting substances, 72 pp. [Available at http://ec.europa. eu/clima/policies/ozone/research/docs/feedstock_en.pdf.] 2012.

Montzka, S.A., Kuijpers, L., Battle, M. O., Aydin, M., Verhulst, K. R., Saltzman, E.S. and Fahey, D. W., Recent increases in global HFC-23 emissions, Geophys. Res, Lett, 37, L02808, doi:10.1029/2009GL041195, 2010.

Mühle, J., Ganesan, A. L., Miller, B. R., Salameh, P. K., Harth, C. M., Greally, B. R., Rigby, M., Porter, L. W., Steele, L. P., Trudinger, C. M., Krummel, P. B., O'Doherty, S., Fraser, P. J., Simmonds, P. G., Prinn, R. G., and Weiss, R. F.: Perfluorocarbons in the global atmosphere: tetrafluoromethane, hexafluoroethane, and octafluoropropane, Atmos. Chem. Phys., 10, 5145–5164, doi:10.5194/acp-10-5145, 2010.

Munnings, C., Leard, B., and Bento, A.: The net emissions impact of HFC-23 offset projects from the Clean Development Mechanism, Resources for the Future, Discussion Paper 16-01, 2016.

Myhre, G., Shindell, D., Bréon, F. M., Collins, W., Fuglestvedt, J., Huang, J., Koch, D., Lamarque, J. F., Lee, D., Mendoza, B., Nakajima, T., Robock, A., Stephens, G., Takemura, T., and Zhang, H.: Anthropogenic and Natural Radiative Forcing, Chapter 8: Climate Change 2013: The Physical Science Basis. Contribution of Working Group I to the Fifth Assessment Report of the Intergovernmental Panel on Climate Change [Stocker, T.F., D. Qin, G.-K. Plattner, M. Tignor, S.K. Allen, J. Boschung, A. Nauels, Y. Xia, V. Bex and P.M. Midgley (eds.)]. Cambridge University Press, Cambridge, United Kingdom and New York, NY, USA, 659-740, 2013.

O'Doherty, S., Cunnold, D., Sturrock, G. A., Ryall, D., Derwent, R. G., Wang, R. H. J., Simmonds, P. G., Fraser, P. J., Weiss, R. F., Salameh, P. K., Miller, B. R., Prinn, R. G.: *In situ* chloroform measurements at AGAGE atmospheric research stations from 1994 –1998, J. Geophys. Res., 106, No. D17, 20,429-20,444, ISSN: 0747-7309, 2001.

O'Doherty, S., Cunnold, D. M., Miller, B. R., Mühle, J., McCulloch, A., Simmonds, P. G., Manning, A. J., Reimann, S., Vollmer, M. K., Greally, B. R., Prinn, R. G., Fraser, P. J., Steele, P., Krummel, P. B., Dunse, B. L., Porter, L. W., Lunder, C. R., Schmidbauer, N., Hermansen, O., Salameh, P. K., Harth, C. M., Wang, R. H. J., and Weiss, R. F.: Global and regional emissions of HFC-125 (CHF_2CF_3) from *in situ* and air archive atmospheric observations at AGAGE and SOGE Observatories, J. Geophys. Res., 114, D23304, 2009.

Oram, D.E., Sturges, W. T., Penkett, S. A., McCulloch, A., and Fraser, P. J.: Growth of fluoroform (CHF_3, HFC-23) in the background atmosphere, Geophys. Res. Lett, 25, 35-38, 1998.

Prinn, R. G., Weiss, R. F., Fraser, P. J., Simmonds, P. G., Cunnold, D. M., Alyea, F. N., O'Doherty, S., Salameh, P. K., Miller, B. R., Huang, J., Wang, R. H. J., Hartley, D. E., Harth, C., Steele, L. P., Sturrock, G., Midgley, P. M., and McCulloch, A.: A history of chemically and radiatively important gases in air deduced from ALE/GAGE/AGAGE, J. Geophys. Res., 105 (D14), 17751-17792, doi: 10.1029/2000JD900141, 2000.

Rigby, M., Ganesan, A.L., and Prinn, R.G.: Deriving emissions time series from sparse atmospheric mole fractions, J. Geophys. Res., 116, D08306, doi:10.1029/2010JD015401, 2011.

Rigby, M., Prinn, R. G., O'Doherty, S., Montzka, S. A., McCulloch, A., Harth, C. M., Mühle, J., Salameh, P. K., Weiss, R. F., Young., D., Simmonds, P. G.: Hall, B. D., Dutton, G. S., Nance, D., Mondeel, D. J., Elkins, J. W., Krummel, P. B., Steele, L. P., and Fraser, P. J.: Re-evaluation of the lifetimes of the major CFCs and CH_3Cl_3 using atmospheric trends, Atmos. Chem. Phys., 13, 1-11, doi:10.5194/acp-13-1-2013, 2013.

Rigby, M., Prinn, R. G., O'Doherty, S., Miller, B. R., Ivy, D., Mühle, J., Harth, C. M., Salameh, P. K., Arnold, T., Weiss, R. F., Krummel, P. B., Steele, P. L., Fraser, P. J., Young., D., and Simmonds, P. G.: Recent and future trends in synthetic greenhouse gas radiative forcing, Geophys. Res. Lett., 41, 2623−2630, 2014.

Rigby, M., Montzka, S. A., Prinn, R. G., White, J. W. C., Young, D., O'Doherty, S., Lunt, M. F., Ganesan, A. L., Manning, A. J., Simmonds, P. G., Salameh, P. K., Harth, C. M., Mühle, J., Weiss, R. F., Fraser, P. J., Steele, L. P., Krummel, P. B., McCulloch, A. and Park, S.: Role of atmospheric oxidation in recent methane growth, Proceedings of the National Academy of Sciences, 201616426, doi:10.1073/pnas.1616426114, 2017

Ruckstuhl, A. F., Henne, S., Reimann, S., Steinbacher, M., Vollmer, M. K., O'Doherty, S., Buchmann, B., and Hueglin, C.: Robust extraction of baseline signal of atmospheric trace species using local regression, Atmos. Meas. Tech., 5, 2613-2624, doi: 10.5194/amt-5-2613-2012, 2012.

Schönenberger, F., Henne, S., Hill, M., Vollmer, M.K., Kouvarakis, G., Mihalopoulos, N., O'Doherty, S., Maione, M., Emmenegger, L., Peter, T., and Reimann, S. Abundance and sources of atmospheric halocarbons in the eastern Mediterranean, Atmos. Chem. Phys. Discuss. 2017. doi.org/10.5194/acp-2017-451.

Simmonds, P. G., M. Rigby, M., McCulloch, A., O'Doherty, S., Young, D., Mühle, J., Krummel, P.B., Steele, L.P., Fraser, P.J., Manning, A.J., Weiss, R. F., Salameh, P. K., Harth, C. M., Wang, R. H. J., and Prinn, R.G.: Changing trends and emissions of hydrochlorofluorocarbons (HCFCs) and their hydrofluorocarbons (HFCs) replacements, Atmos. Chem. Phys. 17, 4641-4655, doi:10.5194/acp-17-4641-2017.

SPARC Report on the Lifetimes of Stratospheric Ozone-Depleting Substances, Their Replacements, and Related Species, edited by Ko, M., Newman, P., Reimann, S., and Strahan, S, SPARC Report No. 6, WCRP-15/2013, 2013.

Spivakovsky, C. M., Logan, J. A., Montzka, S. A., Balkanski, Y. J., Foreman-Fowler, M., Jones, D. B. A., Horowitz, L. W., Fusco, A. C., Brenninkmeijer, C. A. M., Prather, M. J., Wofsy, S. C., and McElroy, M. B.: Three-dimensional climatological distribution of tropospheric OH: Update and evaluation, J. Geophys. Res., 105, 8931–8980, 2000.

Stohl, A., Forster, C., Frank, A., Seibert, P., and Wotawa, G.: Technical note: The Lagrangian particle dispersion model FLEXPART version 6.2, Atmos. Chem. Phys., 5, 2461-2474, doi: 10.5194/acp-5-2461-2005, 2005.

Stohl, A.; Kim, J.; Li, S.; O'Doherty, S.; Mühle, J.; Salameh, P. K.; Saito, T.; Vollmer, M. K.; Wan, D.; Weiss, R. F.; Yao, B.; Yokouchi, Y.; Zhou, L. X.: Hydrochlorofluorocarbon and hydrofluorocarbon emissions in East Asia determined by inverse modelling, Atmos. Chem. Phys. 10, 3545−3560, 2010.

TEAP (Technology and Economic Assessment Panel of the Montreal Protocol), 2006 Assessment Report, United Nations Environment Programme, Nairobi, Kenya, 2006.

Trudinger, C. M., Enting, I. G., Etheridge, D. M., Francey, R. J., Levchenko, V. A., Steele, L. P., Raynaud, D., and Arnaud, L.: Modelling air movement and bubble trapping in firn, J. Geophys. Res., 102, 6747–6763, doi:10.1029/96JD03382, 1997.

Trudinger, C. M., Etheridge, D. M., Rayner, P. J., Enting, I. G., Sturrock, G. A., and Langenfelds, R. L.: Reconstructing atmospheric histories from measurements of air composition in firn, J. Geophys. Res., 107, 4780, doi:10.1029/2002JD002545, 2002.

786 Trudinger, C. M., Enting, I. G., Rayner, P. J., Etheridge, D. M., Buizert, C., Rubino, M.,
787 Krummel, P. B., and Blunier, T.: How well do different tracers constrain the firn diffusivity
788 profile? Atmos. Chem. Phys., 13, doi:10.5194/acp-13-1485-2013, 2013.

789 Trudinger, C. M., Fraser, P. J., Etheridge, D. M., Sturges, W. T., Vollmer, M. K., Rigby, M.,
790 Martinierie, P., Mühle, J. Worton, D. R., Krummel, 15 P. B., Steele, L. P., Miller, B. R., Laube,
791 J., Mani, F., Rayner, P. J., Harth, C. M., Witrant, E., Blunier, T., Schwander, J., O'Doherty, S.,
792 and Battle, M.: Atmospheric abundance and global emissions of perfluorocarbons CF_4, C_2F_6 and
793 C_3F_8 since 1800 inferred from ice core, firn, air archive and *in situ* measurements, Atmos. Chem.
794 Phys., 16, 11 733–11 754, doi:10.5194/acp-16-11733-2016, 2016.

795 UNEP (2009). (United Nations Environment Programme), HCFC Production Data,
796 http://ozone.unep.org/Data_Access/, U.N.Environ. Programme. Nairobi, 2009.

797 UNEP (2017a). Key aspects related to HFC-23 by-product control technologies
798 UNEP./OzL.Pro/ExCom/78/9. 7 March 2017.

799 UNEP (2017b). Production and Consumption of Ozone Depleting Substances under the
800 Montreal Protocol, 1986-2015, United Nations Environment Programme, available at
801 http://ozone.unep.org/en/data-reporting/data-centre

802 UNFCCC (2009). (United Nations Framework Convention on Climate Change), Greenhouse
803 Gas Emissions Data, available at http://unfccc.int/ghg_data/ghg_data_unfccc/items/4146.php,
804 U.N. Framework Conv. on Climate Change, Bonn, Germany, 2009.

805 UNFCCC (2017), Greenhouse Gas Emissions Data, U.N. Framework Conv, on Clim. Change,
806 Bonn, Germany, available at
807 *http://unfccc.int/national_reports/annex_i_ghg_inventories/national_inventories_submissions/it*
808 *ems/10116.php*

809 USEPA, (2013). Global mitigation of non-CO_2 greenhouse gases: 2010-2030, United States
810 Environmental Protection Agency, EPA-430-R-13-011, September 2013.

811 Vollmer, M. K., Mühle, J., Trudinger, C. M., Rigby, M., Montzka, S. A., Harth, C. M., Miller,
812 B. R., Henne, S., Krummel, P. B., Hall, B. D., Young, D., Kim, J., Arduini, J., Wenger, A., Yao,
813 B., Reimann, S., O'Doherty, S., Maione, M., Etheridge, D. M., Li, S., Verdonik, D. P., Park, S.,
814 Dutton, G., Steele, L. P., Lunder, C. R., Rhee, T. S., Hermansen, O., Schmidbauer, N., Wang, R.
815 H. J., Hill, M., Salameh, P. K., Langenfelds, R. L., Zhou, L., Blunier, T., Schwander, J., Elkins,
816 J. W., Butler, J. H., Simmonds, P. G., Weiss, R. F., Prinn, R. G., and Fraser, P. J.: Atmospheric
817 histories and global emissions of halons H-1211 ($CBrClF_2$), H-1301 ($CBrF_3$), and H-2402
818 ($CBrF_2CBrF_2$), J. Geophys. Res. Atmos., 121, 3663–3686, doi:10.1002/2015JD024488, 2016.

819 Vollmer, M. K., Young, D., Trudinger, C.M., Mühle, J., Henne, S., Rigby, M., Park, S., Li, S.,
820 Guillevic, M., Mitrevski, B., Harth, C. M., Miller, B. R., Reimann, S., Yao, B., Steele, L. P.,
821 Wyss, S.A., Lunder, C.R., Arduini, J., McCulloch, A., Wu, S., Rhee, T.S., Wang, R. H. J.,
822 Salameh, P. K., Hermansen, O., Hill, M., Langenfelds, R. L., Ivy, D., O'Doherty, S., Krummel,
823 P. B., Maione, M., Etheridge, D. M., Zhou, L., Fraser, P. J., Prinn, R. G., Weiss, R. F.
824 Simmonds, P. G: Atmospheric histories and emissions of chlorofluorocarbons CFC-13 ($CClF_3$),
825 ΣCFC-114 ($C_2Cl_2F_4$), and CFC-115 (C_2ClF_5), Atmos.Chem. Phys.,18, 979-1002, 2018.

Yao, B., Vollmer, M. K., Zhou, L. X., Henne, S., Reimann, S., Li, P. C., Wenger, A., and Hill, M. 2012.: In-situ measurements of atmospheric hydrofluorocarbons (HFCs) and perfluorocarbons (PFCs) at the Shangdianzi regional background station, China, Atmos. Chem. Phys, 12, 10181-10193; doi:10.5194/acp-12-10181-2012.

Yokouchi, Y; Taguchi, S., Saito, T., Tohjima, Y., Tanimoto, H., and Mukai, H.: High frequency measurements of HFCs at a remote site in East Asia and their implications for Chinese emissions, Geophys. Res. Lett, 33, doi:10.1029/2006GL026403, 2006.

Xiang, B., Prabir, P. K., Montzka, S. A., Miller, S. M., W. Elkins, J. W., Moore, F. L., Atlas, E. L., Miller, B. R., Weiss, R. F., Prinn, R. G. and Wofsy, S. C.: Global emissions of refrigerants HCFC-22 and HFC-134a: Unforeseen seasonal contributions, PNAS 2014 December, 111 (49) 17379-17384. (https://doi.org/10.1073/pnas.1417372111).

Data availability

The entire ALE/GAGE/AGAGE data base comprising every calibrated measurement including pollution events is archived with the Carbon Dioxide Information and Analysis Center (CDIAC) at the U.S. Department of Energy, Oak Ridge National Laboratory (http://cdiac.ornl.gov and also (http://agage.mit.edu/data/agage-data).

Table 1. AGAGE sites used in this study, their coordinates and start dates for GC-MS-Medusa measurements of HFC-23 and HCFC-22.

AGAGE Site	Latitude	Longitude	HFC-23	HCFC-22
Mace Head (MHD), Ireland[1]	53.3° N	9.9° W	Oct. 2007	Nov. 2003
Trinidad Head (THD), California, USA	41.0° N	124.1° W	Sep. 2007	Mar. 2005
Ragged Point (RPB), Barbados	13.2° N	59.4° W	Aug. 2007	May. 2005
Cape Matatula (SMO), American Samoa	14.2° S	170.6° W	Oct. 2007	May. 2006
Cape Grim (CGO), Tasmania, Australia	40.7° S	144.7° E	Nov. 2007	Jan 2004
Jungfraujoch, Switzerland[1]	46.5°N	8.0°E	Apr. 2008	Aug. 2012
Cape Grim Air Archive			Apr. 1978	Apr. 1978

[1] Observations used for regional European emissions

Table 2. Annual mean global HFC-23 emissions, mole fractions, and growth rates, derived from the AGAGE 12-box model.

Year	HFC-23 global annual emissions (Gg yr^{-1}) ±1 sigma (σ) SD.	HFC-23 global mean mole fraction (pmol mol^{-1}) ±1 sigma (σ) SD.	HFC-23 global growth rate (pmol mol^{-1} yr^{-1}) ±1 sigma (σ) SD.
1980	4.2 ± 0.7	3.9 ± 0.1	0.33 ± 0.05
1981	4.2 ± 0.8	4.3 ± 0.1	0.33 ± 0.05
1982	4.4 ± 0.7	4.6 ± 0.1	0.35 ± 0.07
1983	5.2 ± 0.7	5.0 ± 0.1	0.41± 0.05
1984	5.6 ± 0.7	5.4 ± 0.1	0.44 ± 0.05
1985	5.8 ± 0.8	5.9 ± 0.1	0.45± 0.05
1986	5.8 ± 0.7	6.3 ± 0.1	0.45 ± 0.05
1987	5.9 ± 0.7	6.8 ± 0.1	0.46 ± 0.05
1988	6.8 ± 0.7	7.2 ± 0.1	0.52 ± 0.05
1989	7.1 ± 0.7	7.8 ± 0.2	0.55 ± 0.05
1990	7.0 ± 0.7	8.3 ± 0.2	0.54 ± 0.05
1991	7.0 ± 0.7	8.9 ± 0.2	0.54 ± 0.05
1992	7.4 ± 0.6	9.4 ± 0.2	0.57 ± 0.05
1993	7.9 ± 0.6	10.0 ± 0.2	0.61 ± 0.04
1994	8.3 ± 0.7	10.6 ± 0.2	0.64 ± 0.04
1995	8.9 ± 0.6	11.3 ± 0.2	0.69 ± 0.05
1996	9.6 ± 0.6	12.0 ± 0.2	0.74 ± 0.04
1997	10.1 ± 0.6	12.8 ± 0.3	0.77 ± 0.04
1998	10.4 ± 0.7	13.6 ± 0.3	0.79 ± 0.04
1999	10.9 ± 0.7	14.4 ± 0.3	0.82 ± 0.04
2000	10.4 ± 0.8	15.2 ± 0.3	0.76 ± 0.05
2001	9.4 ± 0.7	15.9 ± 0.3	0.68 ± 0.05
2002	9.5 ± 0.7	16.6 ± 0.3	0.69 ± 0.05
2003	10.3 ± 0.8	17.3 ± 0.3	0.77 ± 0.05
2004	11.8 ± 0.8	18.1 ± 0.3	0.90 ± 0.05
2005	13.2 ± 0.8	19.1 ± 0.4	1.01 ± 0.05
2006	13.3 ± 0.8	20.1 ± 0.4	0.99 ± 0.05
2007	11.7 ± 0.7	21.0 ± 0.4	0.85 ± 0.04
2008	11.2 ± 0.6	21.9 ± 0.4	0.78 ± 0.03
2009	9.6 ± 0.6	22.6 ± 0.4	0.68 ± 0.03
2010	10.4 ± 0.6	23.3 ± 0.4	0.74 ± 0.03
2011	11.6 ± 0.6	24.1 ± 0.5	0.85 ± 0.03
2012	12.9 ± 0.6	25.0 ± 0.5	0.96 ± 0.03
2013	14.0 ± 0.6	26.0 ± 0.5	1.04 ± 0.03
2014	14.5 ± 0.6	27.0 ± 0.5	1.05 ± 0.03
2015	13.1 ± 0.7	28.0 ± 0.5	0.95 ± 0.03
2016	12.7 ± 0.6	28.9 ± 0.6	0.94 ± 0.03

Note: Data are tabulated as annual mean mid-year values.

Earlier emissions estimates (1930-1979) determined from the AGAGE 12-box model are listed in Supplementary Material (6), Table S5.

Table 3. Annual mean global HCFC-22 emissions, mole fractions, and growth rates, derived from the AGAGE 12-box model.

Year	HCFC-22 global annual emissions (Gg yr^{-1}) ±1 sigma (σ) SD.	HCFC-22 global mean mole fraction (pmol mol^{-1}) ±1 sigma (σ) SD.	HCFC-22 global growth rate (pmol mol^{-1} yr^{-1}) ±1 sigma (σ) SD.
1980	116.8 ± 17.6	41.6 ± 1.0	4.1 ± 0.9
1981	123.4 ± 18.8	45.8 ± 1.2	4.2 ± 0.8
1982	125.7 ± 15.7	49.9 ± 1.3	4.0 ± 0.8
1983	125.2 ± 20.1	53.7 ± 0.9	3.6 ± 1.0
1984	136.8 ± 18.1	57.3 ± 1.1	4.2 ± 0.6
1985	166.1 ± 17.0	62.2 ± 1.0	5.7 ± 0.7
1986	174.2 ± 19.3	68.5 ± 1.0	5.5 ± 0.7
1987	155.4 ± 20.2	72.9 ± 1.2	4.1 ± 0.7
1988	177.8 ± 19.6	77.2 ± 1.0	5.0 ± 0.7
1989	198.0 ± 19.8	82.9 ± 1.0	6.0 ± 0.7
1990	209.1 ± 19.7	89.1 ± 1.2	6.2 ± 0.6
1991	212.2 ± 21.4	95.1 ± 1.2	5.8 ± 0.7
1992	207.1 ± 23.9	100.5 ± 1.3	5.0 ± 0.6
1993	214.6 ± 22.8	105.4 ± 1.3	5.0 ± 0.6
1994	222.7 ± 22.9	110.4 ± 1.3	5.2 ± 0.5
1995	241.4 ± 26.9	115.9 ± 1.3	5.7 ± 0.5
1996	230.1 ± 24.3	121.4 ± 1.3	4.8 ± 0.5
1997	238.3 ± 24.1	125.8 ± 1.3	5.0 ± 0.5
1998	256.0 ± 27.2	131.7 ± 1.3	5.7 ± 0.4
1999	251.8 ± 28.4	136.8 ± 1.4	5.0 ± 0.3
2000	275.1 ± 28.7	142.0 ± 1.4	5.8 ± 0.2
2001	275.3 ± 28.8	147.9 ± 1.5	5.5 ± 0.2
2002	280.7 ± 31.6	153.1 ± 1.6	5.3 ± 0.2
2003	286.3 ± 30.1	158.3 ± 1.6	5.3 ± 0.2
2004	292.1 ± 30.6	163.7 ± 1.7	5.3 ± 0.2
2005	312.3 ± 34.6	169.2 ± 1.6	6.1 ± 0.2
2006	334.3 ± 35.0	175.9 ± 1.7	7.2 ± 0.2
2007	355.6 ± 35.2	183.6 ± 1.8	8.0 ± 0.2
2008	372.9 ± 38.4	191.9 ± 1.9	7.9 ± 0.2
2009	368.6 ± 39.7	199.2 ± 2.0	7.4 ± 0.2
2010	385.8 ± 41.3	206.8 ± 2.0	7.4 ± 0.3
2011	373.1 ± 41.3	213.7 ± 2.1	6.2 ± 0.2
2012	373.2 ± 45.5	219.3 ± 2.2	5.5 ± 0.2
2013	369.6 ± 44.1	224.7 ± 2.3	5.0 ± 0.2
2014	373.9 ± 45.7	229.5 ± 2.3	4.6 ± 0.2
2015	364.2 ± 47.7	233.7 ± 2.2	3.9 ± 0.2
2016	370.3 ± 45.9	237.5 ± 2.2	3.9 ± 0.2

Note: Data are tabulated as annual mean mid-year values. These HCFC-22 global emissions estimates are updates of the HCFC-22 emissions reported in Simmonds et al. (2017) for the period 1995-2015.

Table 4: European HFC-23 emissions (tonne, Mg) by country/region: E_a *a priori*, E_b *a posteriori* emissions, f_a fraction of *a priori* emissions from factory locations, f_b fraction of *a posteriori* emissions from factory locations. All values represent averages from both inversions using different *a priori* distributions.

	Germany				**France**				**Italy**			
year	E_a (Mg/yr)	E_b (Mg/yr)	f_a (%)	f_b (%)	E_a (Mg/yr)	E_b (Mg/yr)	f_a (%)	f_b (%)	E_a (Mg/yr)	E_b (Mg/yr)	f_a (%)	f_b (%)
2009	8±16	34±12	30	49	15±31	2±3.2	88	6	8.4±17	34±8.7	26	52
2010	7.6±15	19±14	27	13	12±23	15±5.1	84	86	9±18	48±9.3	26	45
2011	8±16	44±13	33	58	7.7±15	10±3.4	70	73	9.2±18	34±11	26	43
2012	7.6±15	32±9.7	30	40	8.1±16	8.3±3.4	76	73	9.1±18	25±8.6	26	31
2013	7.2±14	16±9.4	28	58	9.2±18	27±16	82	93	9.3±19	47±24	26	29
2014	7.1±14	20±9.2	30	27	9.4±19	10±2.3	84	85	9.5±19	32±14	26	32
2015	6.6±13	12±8.7	29	14	9.5±19	17±3.9	86	92	9.8±20	37±19	26	24
2016	6.6±13	19±9.1	29	26	9.5±19	9.9±3.4	86	85	9.8±20	23±10	26	39

	Benelux				**United Kingdom**				**Iberian Peninsula**			
year	E_a (Mg/yr)	E_b (Mg/yr)	f_a (%)	f_b (%)	E_a (Mg/yr)	E_b (Mg/yr)	f_a (%)	f_b (%)	E_a (Mg/yr)	E_b (Mg/yr)	f_a (%)	f_b (%)
2009	13±27	25±8.8	98	99	3.8±7.6	5.3±3.1	84	87	97±190	56±29	57	10
2010	34±67	16±7.1	99	98	1.2±2.3	2.8±1.9	48	71	130±260	120±33	66	52
2011	15±29	21±16	97	97	1±2.1	1.5±1.7	39	21	83±170	75±27	50	27
2012	11±22	53±13	96	99	0.92±1.8	2±1.6	26	46	74±150	46±27	45	43
2013	16±33	94±13	98	100	1.1±2.1	2.1±1.8	29	48	64±130	110±27	38	22
2014	3.8±7.6	11±6.3	85	94	1.3±2.5	6.8±2.4	35	73	59±120	55±27	35	45
2015	8.7±17	20±12	94	97	1.4±2.7	2.5±2.1	34	37	48±96	19±18	26	9
2016	8.7±17	45±11	94	99	1.4±2.7	3.8±2.2	34	42	48±96	69±24	26	33

Note : **Benelux** (Belgium, the Netherlands, and Luxembourg).

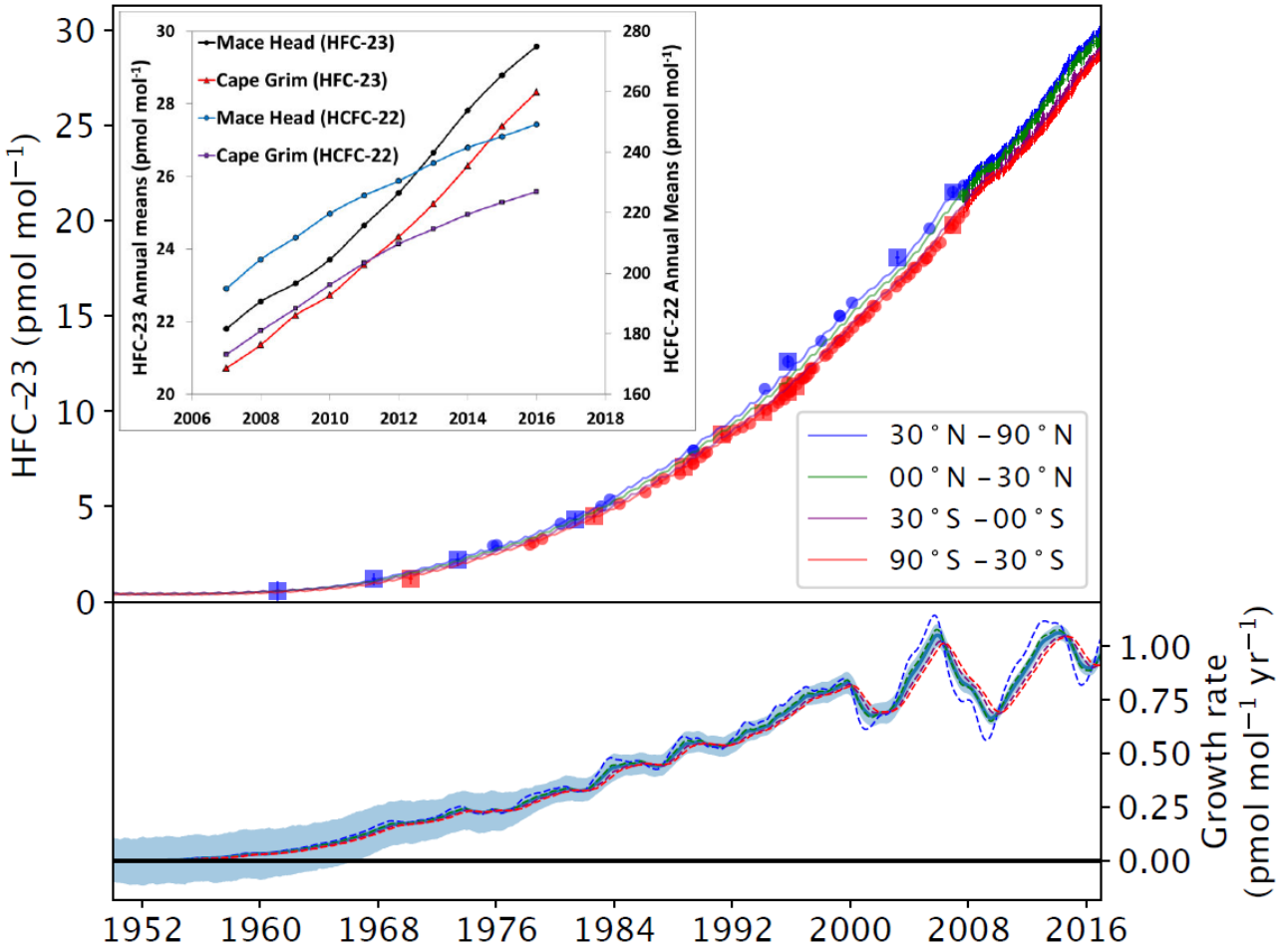

Figure 1. HFC-23 modelled mole fractions for the four equal-mass latitudinal subdivisions of the global atmosphere calculated from the 12-box model and the *in situ* records from the AGAGE core sites (points with error bars), firn air (squares, red SH, blue NH), old NH air data (blue circles, only shown for times without NH *in situ* data), and CGAA data (red circles, only shown for times without SH in situ data). Lower box shows the annual growth rates (global – blue solid line with uncertainty band - and individual semi-hemispheres – dashed lines) in pmol mol^{-1} yr^{-1}. Figure 1 inset, compares the annual mean mole fractions of HFC-23 and HCFC-22 recorded at Mace Head and Cape Grim from 2007-2016.

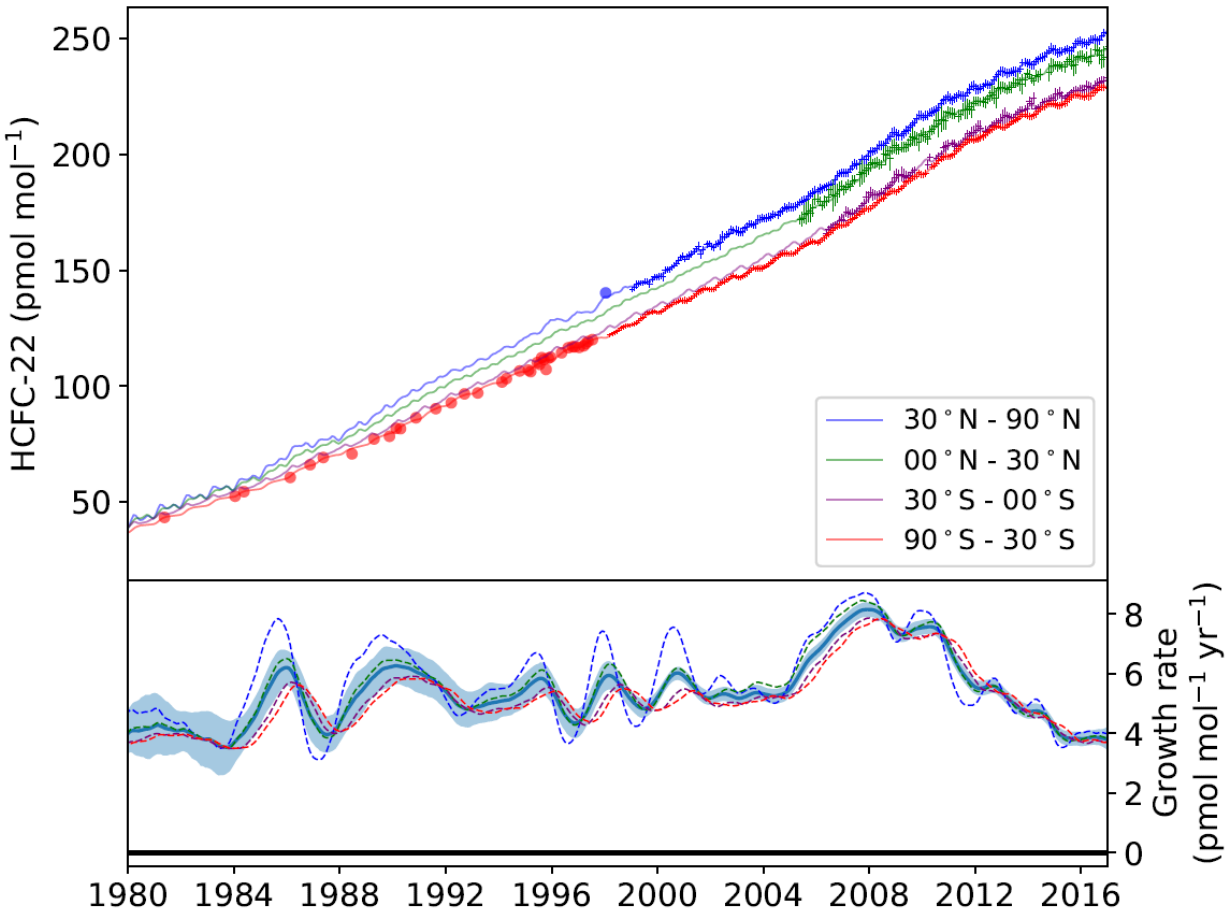

Figure 2. HCFC-22 modelled mole fractions for the four equal-mass latitudinal subdivisions of the global atmosphere calculated from the 12-box model and the *in situ* records from the AGAGE core sites (points with error bars) and CGAA data (red circles, only shown for times without *in situ* data) and old NH air data (blue circles, only shown for times without NH *in situ* data). Lower box shows the annual growth rates (global – blue solid line with uncertainty band - and individual semi-hemispheres – dashed lines) in pmol mol^{-1} yr^{-1}.

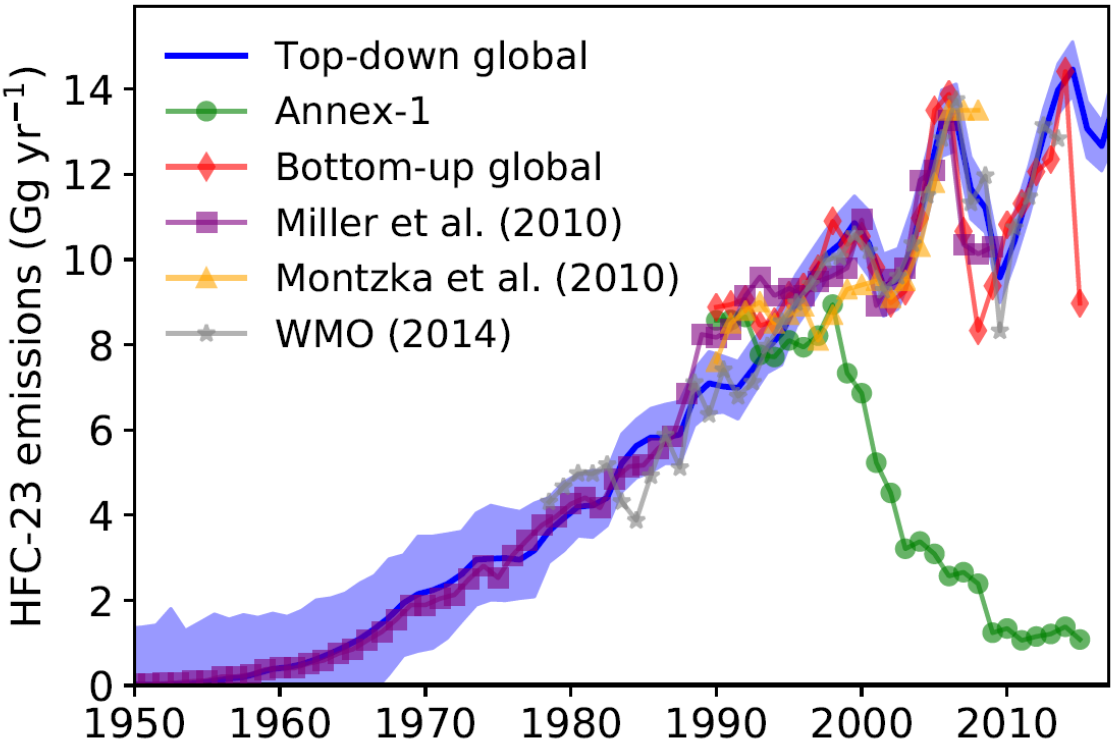

Figure 3. Global emissions of HFC-23 calculated from the AGAGE 12-box model (blue line and shading, 1 σ uncertainty). Data are plotted as annual mean values, centred on the middle of each year. The purple line shows bottom-up HFC-23 estimates of emissions from Miller et al. (2010), the yellow line HFC-23 emissions estimates from Montzka et al. (2010) and the grey line from Carpenter and Reimann (WMO 2014). The green line shows emissions reports by Annex-1 countries. The red line shows the bottom-up estimated global emissions developed here and discussed in (Supplementary Material 3).

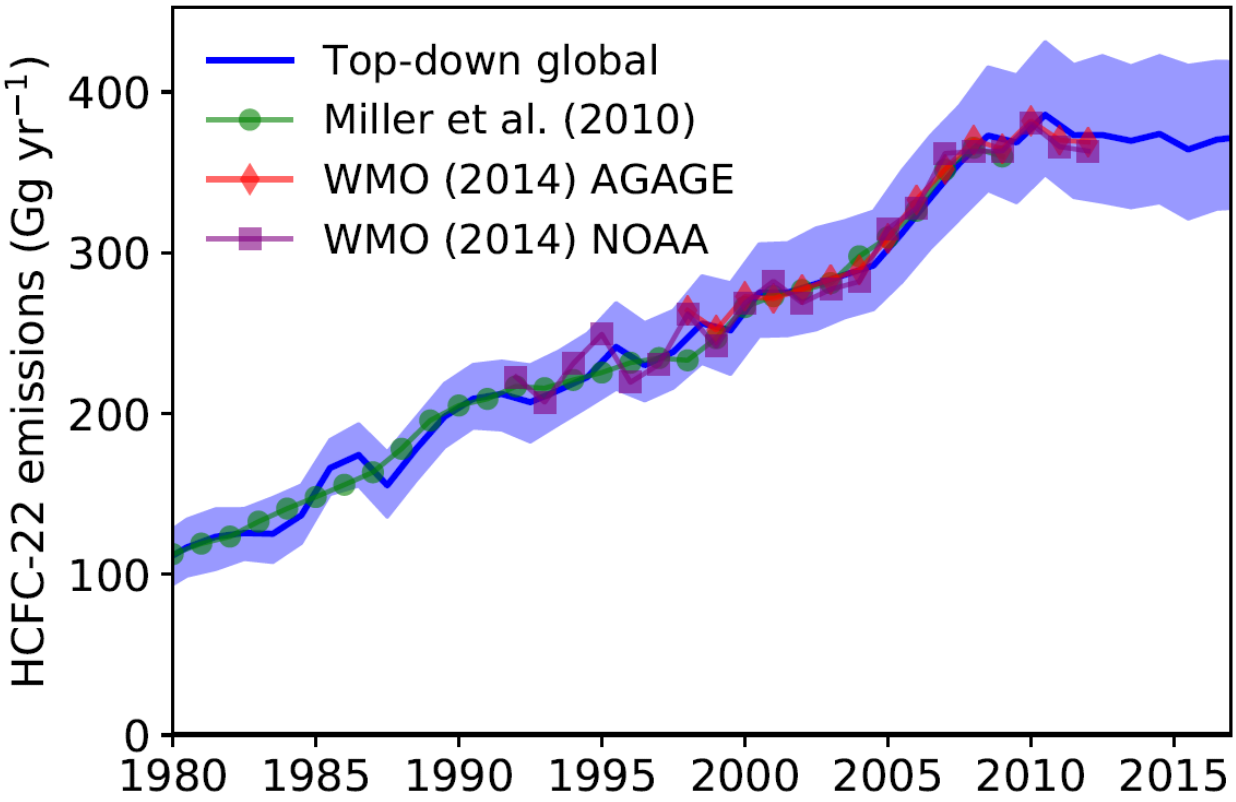

Figure 4. Global emissions of HCFC-22 calculated from the AGAGE 12-box model (blue line and shading, 1σ uncertainty). Data are plotted as annual mean mid-year values. The green line shows bottom-up HCFC-22 estimates of emissions from Miller et al. (2010). Red and purple lines show HCFC-22 emissions calculated from AGAGE and NOAA data/models respectively, reported in WMO 2014 (Carpenter and Reimann, 2014).

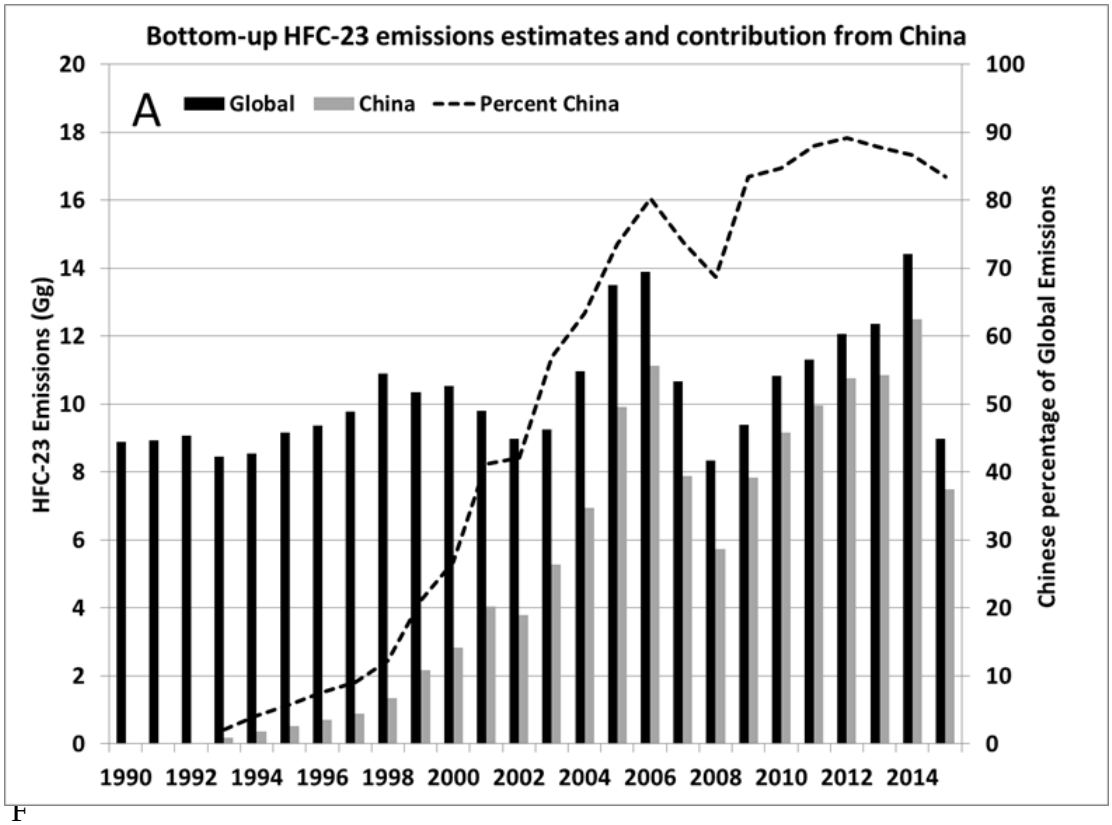

F

Figure 5a. HFC-23 global and Chinese emissions estimates and the percentage of Chinese emissions contributing to the global total (dashed line). Compiled from Table S4 in Supplementary Material (3).

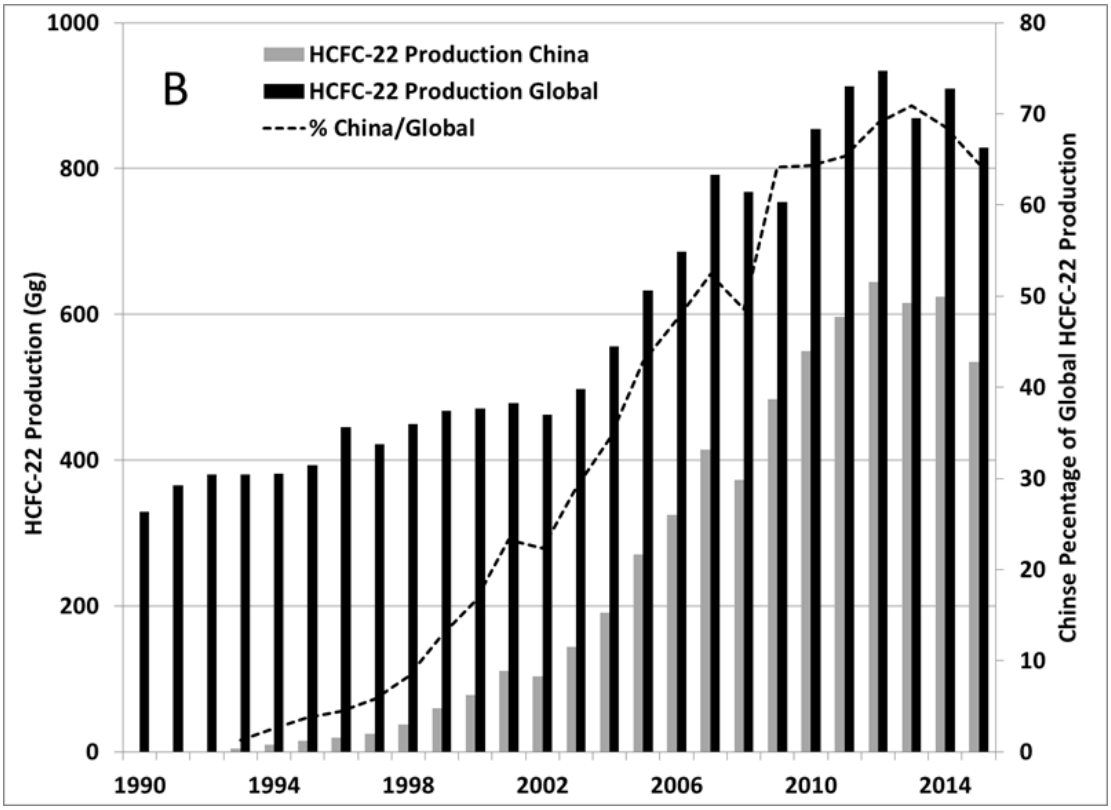

Figure 5b. HCFC-22 emissions estimates of global and Chinese production and the percentage of Chinese production as a fraction of the global total (dashed line). Compiled from Table S3 in Supplementary Material (3).

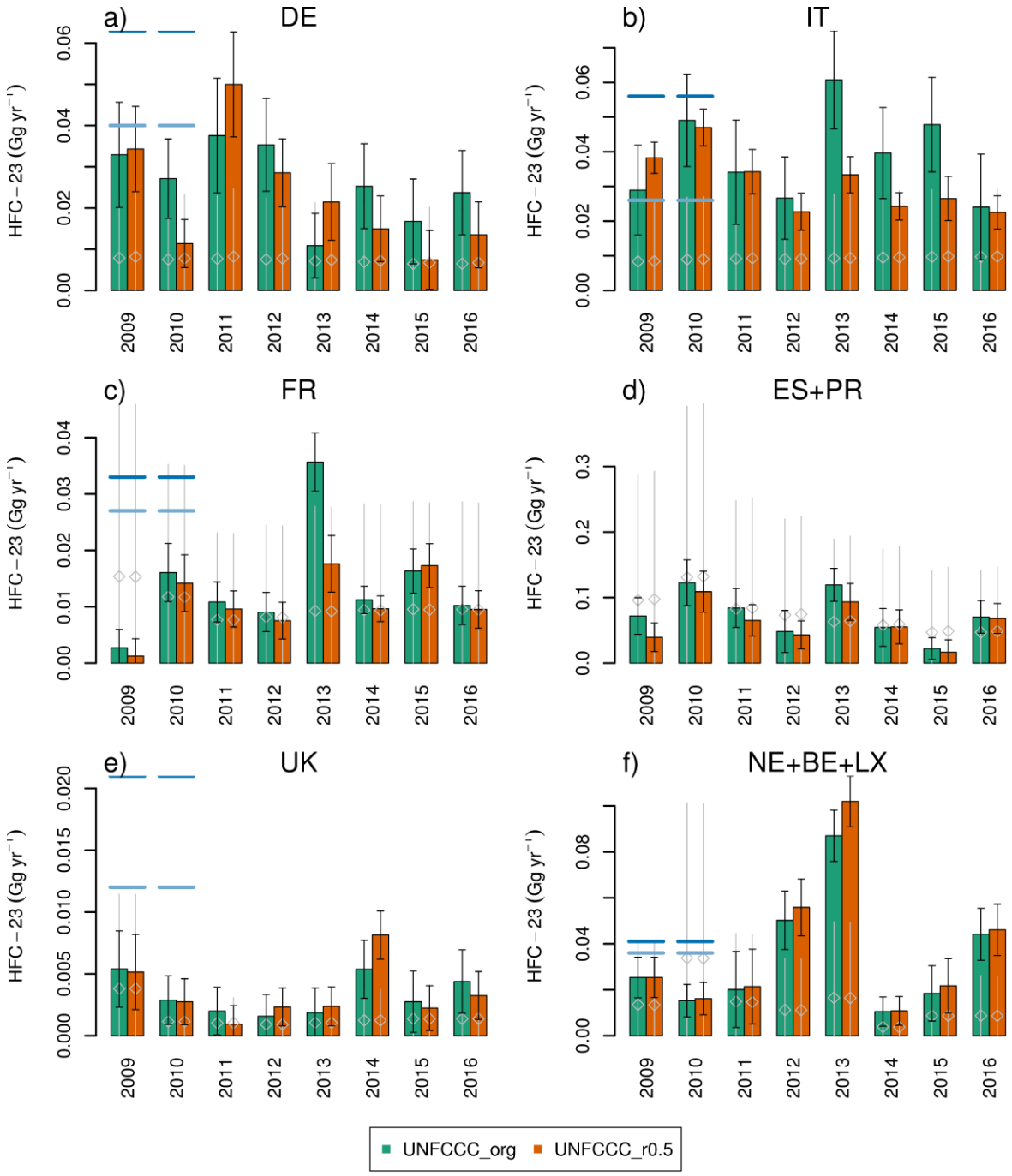

Figure 6: Temporal evolution of national/regional emissions of HFC-23: solid bars and error bars give *a posteriori* emissions using the two sets of *a priori* emissions (grey lines). The two approaches (green and orange bars) spatially distribute these different bottom-up estimates (see section 2.7.3). Blue horizontal lines give the estimates of Keller et al. (2011) for their Bayesian (light blue) and point source (dark blue) estimate; a) Germany (DE), b) Italy (IT), c) France (FR), d) Spain and Portugal (ES+PR), e) United Kingdom (UK), f) Benelux countries (Netherlands, Belgium, Luxembourg, NE+BE+LX).

Supplementary Material

Recent increases in the growth rate and emissions of HFC-23 (CHF_3) and the link to HCFC-22 ($CHClF_2$) production

Peter G. Simmonds[1], Matthew Rigby[1], Archie McCulloch[1], Martin K. Vollmer[2], Stephan Henne[2], Jens Mühle[3], Simon O'Doherty[1], Alistair J. Manning[4], Paul B. Krummel[5], Paul J. Fraser[5], Dickon Young[1], Ray F. Weiss[3], Peter K. Salameh[3], Christina M. Harth[3], Stefan Reimann[2], Cathy M. Trudinger[5], L. Paul Steele[5], Ray H. J. Wang[6], Diane J. Ivy[7], Ronald G. Prinn[7], Blagoj Mitrevski[5], and David M. Etheridge[5].

[1] Atmospheric Chemistry Research Group, University of Bristol, Bristol, UK
[2] Swiss Federal Laboratories for Materials Science and Technology, Laboratory for Air Pollution and Environmental Technology (Empa), Dübendorf, Switzerland,
[3] Scripps Institution of Oceanography (SIO), University of California at San Diego, La Jolla, California, USA
[4] Met Office Hadley Centre, Exeter, UK
[5] Climate Science Centre, Commonwealth Scientific and Industrial Research Organisation (CSIRO) Oceans and Atmosphere, Aspendale, Victoria, Australia
[6] School of Earth, and Atmospheric Sciences, Georgia Institute of Technology, Atlanta, Georgia, USA
[7] Center for Global Change Science, Massachusetts Institute of Technology, Cambridge, Massachusetts, USA

Correspondence to: P.G. Simmonds (petergsimmonds@aol.com)

Supplementary Material (1): AGAGE Instrumentation and Measurement Techniques

Typically for each measurement, the analytes from two litres of air are collected on the microtrap and, after fractionated distillation, purification and transfer, are desorbed onto a single main capillary chromatography column (CP-PoraBOND Q, 0.32 mm ID × 25 m, 5 μm, Agilent Varian Chrompack, batch-made for AGAGE applications) purged with helium (research grade 6.0) that is further purified using a heated helium purifier (HP2, VICI, USA). Separation and detection of the compounds are achieved by using Agilent Technology GCs (model 6890N) and quadrupole mass spectrometers in selected ion mode (initially model 5973 series, progressively converted to 5975C over the later years).

The quaternary standards are whole-air samples, pressurized into 34 L internally electropolished stainless steel canisters (Essex Industries, USA). They are filled by the responsible station scientist and/or on-site station personnel who are in charge of the respective AGAGE remote sites using modified oil-free diving compressors (SA-3 and SA-6, RIX Industries, USA) to ~60 bar (older canisters to ~40 bar). Cape Grim is an exception, where the canisters used for quaternary standard purposes are filled cryogenically. This method of cryogenically collecting large volumes of ambient air is the same as that is used for collecting air for the CGAA and measurements of many atmospheric trace species in air samples collected in

this manner show that the trace gas composition of the air is well preserved (Fraser et al., 1991, 2016; Langenfelds et al., 1996, 2003). The on-site quaternary standards are compared weekly to tertiary standards from the central calibration facility at the Scripps Institution of Oceanography (SIO) in order to propagate the primary calibration scales and assess any long-term drifts. These tertiary standards are filled with ambient air in Essex canisters under "baseline" clean air conditions at Trinidad Head or at La Jolla (California) and are measured at SIO against secondary ambient air standards (to obtain an "out" value) before they are shipped to individual AGAGE sites. We define "baseline" as air masses that are representative of the unpolluted marine boundary layer, uninfluenced by recent local or regional emissions. After their on-site deployment they are again measured at SIO to obtain an "in" value, to assess any possible drifts. They are also measured on-site against the previous and next tertiaries. The secondary standards and the synthetic primary standards at SIO provide the core of the AGAGE calibration system (Prinn et al., 2000; Miller et al., 2008).

The GC-MS-Medusa measurement precisions for HFC-23 and HCFC-22 are determined as the precisions of replicate measurements of the quaternary standards over twice the time interval as for sample-standard comparisons (Miller et al., 2008). Accordingly, they are upper-limit estimates of the precisions of the sample-standard comparisons. Typical daily precisions for each compound vary with abundance and individual instrument performance over time. Average percentage relative standard deviation (% RSD) between 2007 and 2016 were: HFC-23 (0.1%-1.9%, average 0.7%); and for HCFC-22 (0.1%-2.5%, average 0.6%).

Supplementary Material (2): Firn Air Depth Profiles, Analyses of the CGAA and old Northern Hemisphere (NH) air samples

In this section we illustrate in Figures S1 the depth profiles for HFC-23 in the polar firn and in Figure S2 we show three independent analyses of the data from the CGAA. Tables S1 and S2 also list the actual data used to construct these figures.

Figure S1. Depth profiles for HFC-23 in polar firn. DSSW20K and SPO-01 are Antarctic sites and NEEM-08 is from Greenland. The modelled mole fractions correspond to the optimized emissions history using an inversion and firn air model developed at CSIRO.

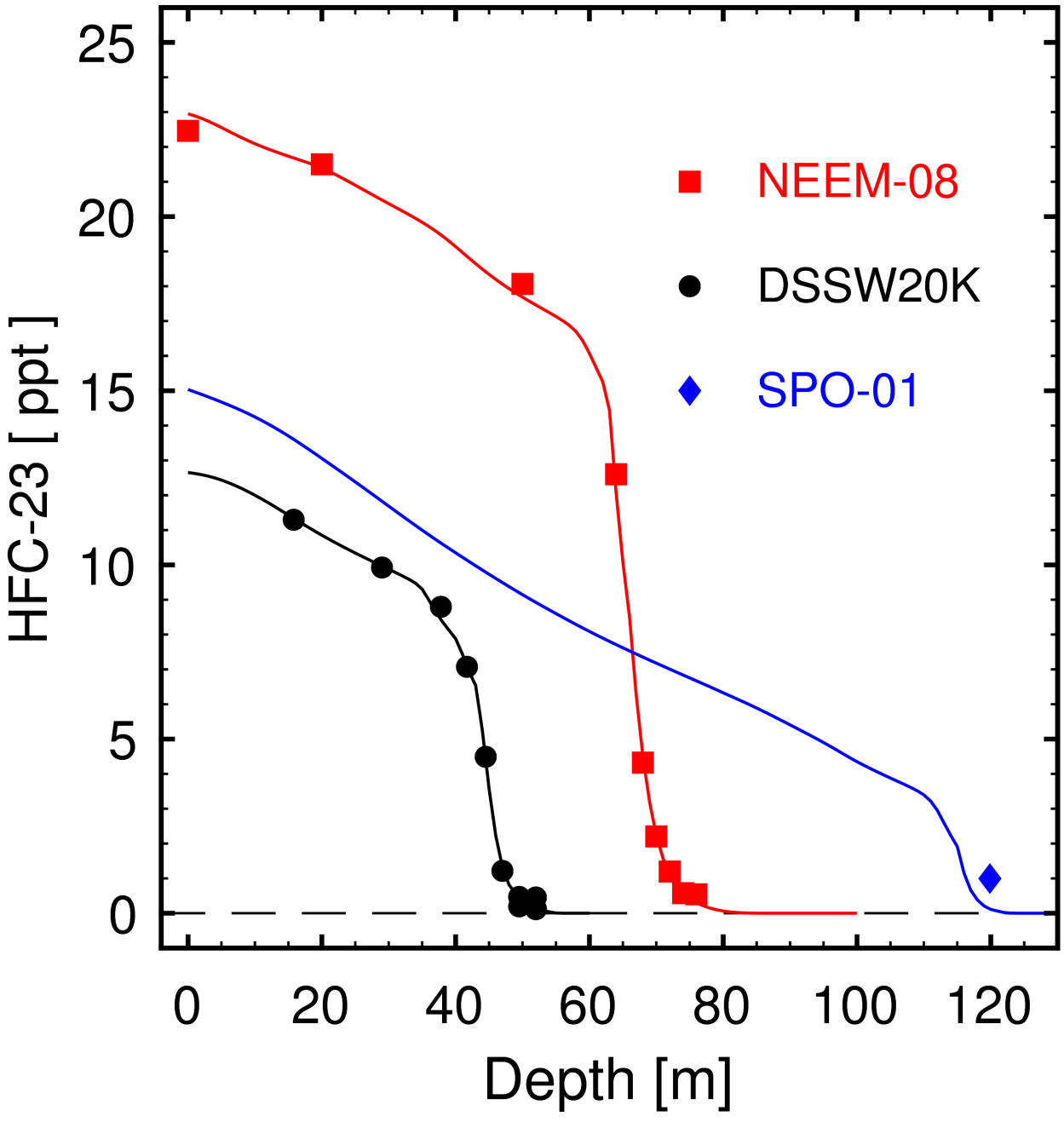

Figure S2. Comparison of three analysis sets of HFC-23 in the Cape Grim Air Archive

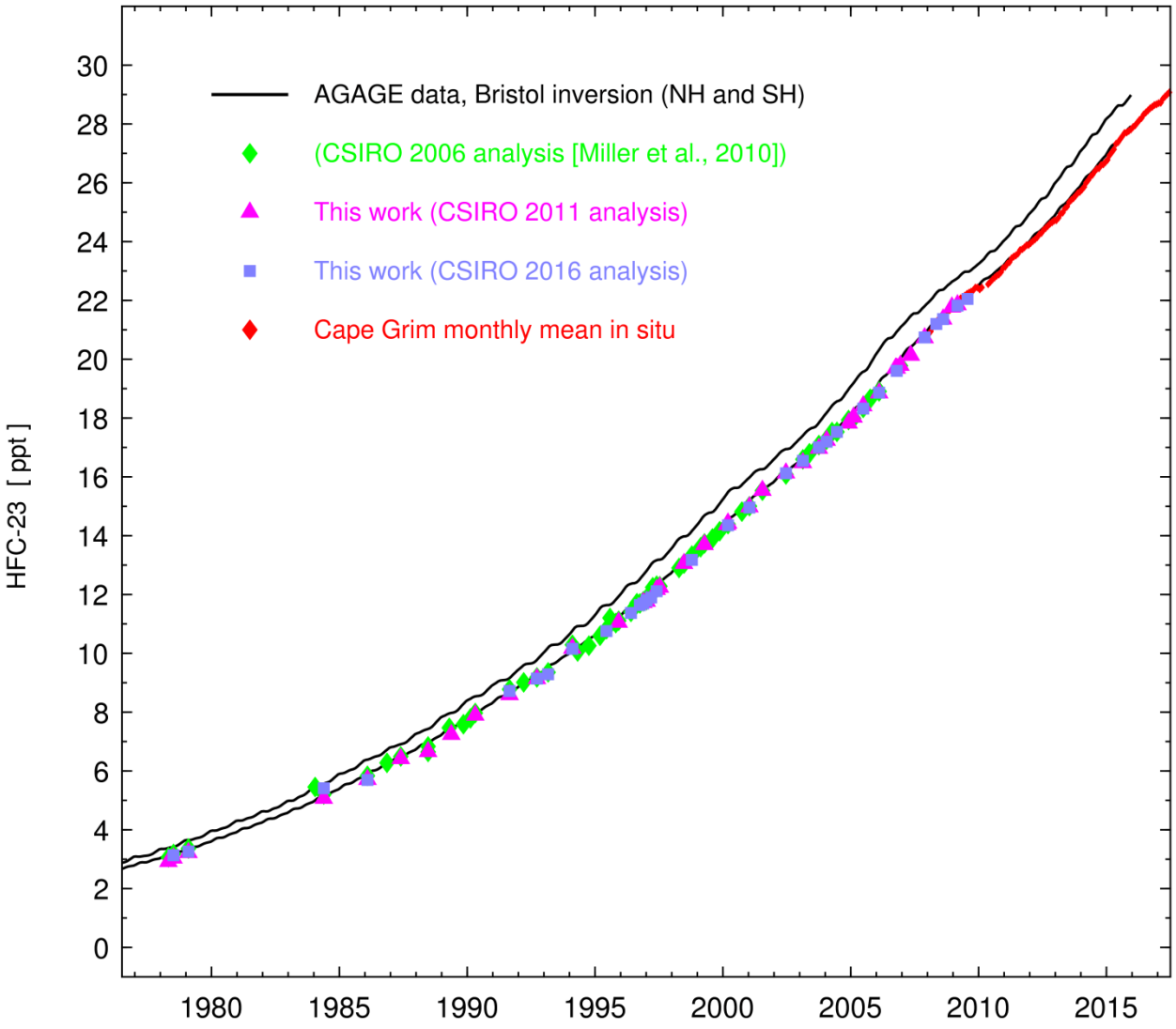

A series of old Northern Hemisphere (NH) air samples were mostly collected during clean air conditions but not with the purpose of creating a consistent air archive. Therefore, a stepwise tightening filtering algorithm was applied to the measurement results based on their deviations from a fit through all data (including in situ data). Due to the scarcity of the Northern Hemisphere HFC-23 data, the filtering of these samples used the fit through the filtered Southern Hemisphere samples as additional guide (with an appropriate time lag related to hemispheric transport). The remaining final NH HFC-23 data showed good agreement with concurrent in situ measurements. (Mühle et al., 2010; Vollmer et al., 2016)

Table S1

Firn air measurement and model results for HFC-23

Abbreviations: m: measured; mf: mole fraction; p: precision (measurement repeatability, 1 sigma); mod: firn air model output with uncertainties

Primary calibration scale for HFC-23: SIO-07

depth: depth in firn air hole from which sample was drawn

Sample Volume: volume of sample used in one analysis on the Medusa-GCMS

Flags used for the decisions on presence of the compound in the sample

Flag 1: Peak size large enough a non-zero positive mole fraction was calculated and reported.

Flag 2: Clear sign of a peak but very small. Mole fraction was calculated by GCWerks either using generally set parameters or using GCWerks special integration

Flag 3: Maybe a peak some baseline disturbance that point to a non-zero signal. In most cases a mole fraction assigned

Flag 4: no sign of a peak at all no change in baseline. Mole fraction definitely smaller than the estimated detection limit for that sample

					sample	HFC-23								
Site	Tank_ID	UAN	Parent_UAN	depth	volume	m-mf	m-p	n	Flag	mod-mf	mod-min	mod-max	mean Age	effect Age
				[m]	[L]	[ppt]	[ppt]			[ppt]	[ppt]	[ppt]		
DSSW20K	S22L-002	UAN980141	UAN980141	15.8	3	11.295	0.071	3	1	11.335	11.282	11.449	1995.95	1996.26
DSSW20K	MC-05	UAN980780	UAN980142	29	2	9.924	0.098	2	1	9.968	9.856	10.1	1993.63	1994.04
DSSW20K	CA01674	UAN980143	UAN980143	37.8	3	8.796	0.041	4	1	8.431	8.327	8.624	1990.64	1991.23
DSSW20K	MC-08	UAN980783	UAN980144	41.7	2	7.074	0.06	2	1	7.075	6.954	7.307	1987.71	1988.85

DSSW20K	MC-09	UAN980784	UAN980145	44.5	2	4.49	0.018	2	1	4.425	4.221	4.54	1980.51	1982.51
DSSW20K	MC-06	UAN980781	UAN980146	47	2	1.215	0.021	2	1	1.323	1.195	1.411	1966.83	1970.73
DSSW20K	MC-04	UAN980779	UAN980147	49.5	2	0.196	0.033	2	1	0.478	0.414	0.53	1952.95	1953.44
DSSW20K	S22L-010	UAN980148	UAN980148	49.5	1.5	0.468	0.061	2	1	0.478	0.414	0.53	1952.95	1953.44
DSSW20K	MC-01	UAN980776	UAN980150	52	2	0.128	0.011	2	1	0.478	0.414	0.53	1952.95	1953.44
DSSW20K	MC-10	UAN980785	UAN980149	52	1	0.451	0.064	2	1	0.478	0.414	0.53	1952.95	1953.44
DSSW20K	S22L-007	UAN980151	UAN980151	52	2	0.115	0	1	1	0.137	0.137	0.292	1938.93	1937.62
NEEM-2008	S300-B15	UAN999698	UAN999698	0	1.5	22.462	0.104	2	1	0.137	0.137	0.292	1938.93	1937.62
NEEM-2008	S300-B13	UAN999697	UAN999697	20	1.5	21.502	0.189	2	1	0.137	0.137	0.292	1938.93	1937.62
NEEM-2008	S300-B11	UAN999695	UAN999695	50	1.5	18.067	0.067	2	1	0.137	0.137	0.292	1938.93	1937.62
NEEM-2008	S300-B12	UAN999696	UAN999696	64	1.5	12.602	0.1	2	1	0.137	0.137	0.292	1938.93	1937.62
NEEM-2008	S300-B16	UAN999699	UAN999699	68	1.5	4.322	0.012	2	1	0.137	0.137	0.292	1938.93	1937.62
NEEM-2008	S300-B18	UAN999701	UAN999701	70	1.5	2.204	0.051	2	1	0.137	0.137	0.292	1938.93	1937.62
NEEM-2008	S300-B19	UAN999702	UAN999702	72	1.5	1.196	0.047	2	1	0.137	0.137	0.292	1938.93	1937.62
NEEM-2008	S300-B17	UAN999700	UAN999700	74	1.5	0.575	0.05	2	1	0.137	0.137	0.292	1938.93	1937.62
NEEM-2008	S300-B20	UAN999703	UAN999703	76	1.5	0.541	0.011	2	1	NaN	NaN	NaN	NaN	NaN
SPO	S300-A23	UAN996580	UAN993582	119.87	1	0.994	0.04	2	1	21.391	21.182	21.537	2006.96	2007

Table S1

Firn air measurement and model results for HFC-23

Abbreviations: m: measured; mf: mole fraction; p: precision (measurement repeatability, 1 sigma); mod: firn air model output with uncertainties

Primary calibration scale for HFC-23: SIO-07

depth: depth in firn air hole from which sample was drawn

Sample Volume: volume of sample used in one analysis on the Medusa-GCMS

Flags used for the decisions on presence of the compound in the sample

Flag 1: Peak size large enough a non-zero positive mole fraction was calculated and reported.

Flag 2: Clear sign of a peak but very small. Mole fraction was calculated by GCWerks either using generally set parameters or using GCWerks special integration

Flag 3: Maybe a peak some baseline disturbance that point to a non-zero signal. In most cases a mole fraction assigned

Flag 4: no sign of a peak at all no change in baseline. Mole fraction definitely smaller than the estimated detection limit for that sample

					sample	HFC-23								
Site	Tank_ID	UAN	Parent_UAN	depth	volume	m-mf	m-p	n	Flag	mod-mf	mod-min	mod-max	mean	effect
				[m]	[L]	[ppt]	[ppt]			[ppt]	[ppt]	[ppt]	Age	Age
DSSW20K	S22L-002	UAN980141	UAN980141	15.8	3	11.295	0.071	3	1	11.335	11.282	11.449	1995.95	1996.26
DSSW20K	MC-05	UAN980780	UAN980142	29	2	9.924	0.098	2	1	9.968	9.856	10.1	1993.63	1994.04
DSSW20K	CA01674	UAN980143	UAN980143	37.8	3	8.796	0.041	4	1	8.431	8.327	8.624	1990.64	1991.23
DSSW20K	MC-08	UAN980783	UAN980144	41.7	2	7.074	0.06	2	1	7.075	6.954	7.307	1987.71	1988.85

DSSW20K	MC-09	UAN980784	UAN980145	44.5	2	4.49	0.018	2	1	4.425	4.221	4.54	1980.51	1982.51
DSSW20K	MC-06	UAN980781	UAN980146	47	2	1.215	0.021	2	1	1.323	1.195	1.411	1966.83	1970.73
DSSW20K	MC-04	UAN980779	UAN980147	49.5	2	0.196	0.033	2	1	0.478	0.414	0.53	1952.95	1953.44
DSSW20K	S22L-010	UAN980148	UAN980148	49.5	1.5	0.468	0.061	2	1	0.478	0.414	0.53	1952.95	1953.44
DSSW20K	MC-01	UAN980776	UAN980150	52	2	0.128	0.011	2	1	0.478	0.414	0.53	1952.95	1953.44
DSSW20K	MC-10	UAN980785	UAN980149	52	1	0.451	0.064	2	1	0.478	0.414	0.53	1952.95	1953.44
DSSW20K	S22L-007	UAN980151	UAN980151	52	2	0.115	0	1	1	0.137	0.137	0.292	1938.93	1937.62
NEEM-2008	S300-B15	UAN999698	UAN999698	0	1.5	22.462	0.104	2	1	0.137	0.137	0.292	1938.93	1937.62
NEEM-2008	S300-B13	UAN999697	UAN999697	20	1.5	21.502	0.189	2	1	0.137	0.137	0.292	1938.93	1937.62
NEEM-2008	S300-B11	UAN999695	UAN999695	50	1.5	18.067	0.067	2	1	0.137	0.137	0.292	1938.93	1937.62
NEEM-2008	S300-B12	UAN999696	UAN999696	64	1.5	12.602	0.1	2	1	0.137	0.137	0.292	1938.93	1937.62
NEEM-2008	S300-B16	UAN999699	UAN999699	68	1.5	4.322	0.012	2	1	0.137	0.137	0.292	1938.93	1937.62
NEEM-2008	S300-B18	UAN999701	UAN999701	70	1.5	2.204	0.051	2	1	0.137	0.137	0.292	1938.93	1937.62
NEEM-2008	S300-B19	UAN999702	UAN999702	72	1.5	1.196	0.047	2	1	0.137	0.137	0.292	1938.93	1937.62
NEEM-2008	S300-B17	UAN999700	UAN999700	74	1.5	0.575	0.05	2	1	0.137	0.137	0.292	1938.93	1937.62
NEEM-2008	S300-B20	UAN999703	UAN999703	76	1.5	0.541	0.011	2	1	NaN	NaN	NaN	NaN	NaN
SPO	S300-A23	UAN996580	UAN993582	119.87	1	0.994	0.04	2	1	21.391	21.182	21.537	2006.96	2007

Table S2

Cape Grim Air Archive (CGAA) Results for HFC-23 from three analysis periods

Results are reported as dry air mole fractions for abundance (c) and precisions (p)

Measurements are conducted on the CSIRO Aspendale-9 GCMS-Medusa

Primary calibration scales: CFC-23: SIO-07

Notes for 2006: Measurements by B. R. Miller, L. Porter, L. P. Steele, P. B. Krummel. Results by peak area. Standard is G-141 with assigned values: CFC-23: 19.648 ppt

Notes for 2011: Measurements by D. Ivy, L. P. Steele, P. B. Krummel, M. Leist, Results by peak area. Standard is G-181 with assigned values: CFC-23: 23.1456 ppt

Notes for 2016: Measurements by M. K. Vollmer, L. P. Steele, B. Mitrevski, P. B. Krummel, Results by peak area. Standard is E-146S with assigned values: CFC-23: 31.4808 ppt

sampleID	time fractional	year	month	day	c_mean [ppt]	p_mean [ppt]	c_2006 [ppt]	p_2006 [ppt]	n_2006	c_2011 [ppt]	p_2011 [ppt]	n_2011	c_2016 [ppt]	p_2016 [ppt]	n_2016
UAN780001	1978.315	1978	4	26	2.992	0.081	3.065	0.114	3	2.918	0.048	3	NaN	NaN	NaN
UAN780002	1978.512	1978	7	7	3.116	0.018	3.178	0.023	3	3.037	0.009	3	3.133	0.023	3
UAN790001	1979.099	1979	2	6	3.282	0.025	3.363	0.027	3	3.223	0.04	3	3.259	0.008	3
UAN910377	1984.053	1984	1	20	5.453	0.044	5.453	0.044	2	NaN	NaN	NaN	NaN	NaN	NaN
UAN840004	1984.391	1984	5	23	5.226	0.023	5.2	0.034	4	5.066	0.021	4	5.411	0.014	3
UAN860001	1986.099	1986	2	6	5.746	0.048	5.835	0.046	4	5.71	0.086	4	5.694	0.012	3
UAN860005	1986.863	1986	11	12	6.275	0.142	6.275	0.142	4	NaN	NaN	NaN	NaN	NaN	3

UAN870006	1987.403	1987	5	28	6.456	0.06	6.493	0.039	4	6.418	0.08	6	NaN	NaN	NaN
UAN880003	1988.47	1988	6	21	6.651	0.058	6.646	0.065	6	6.657	0.051	3	NaN	NaN	NaN
UAN880002	1988.47	1988	6	21	6.834	0.037	6.834	0.037	4	NaN	NaN	NaN	NaN	NaN	3
UAN890002	1989.299	1989	4	20	7.466	0.04	7.466	0.04	4	NaN	NaN	NaN	NaN	NaN	NaN
UAN890004	1989.378	1989	5	19	7.24	0.083	NaN	NaN	NaN	7.24	0.083	8	NaN	NaN	3
UAN890005	1989.852	1989	11	8	7.589	0.064	7.589	0.064	4	NaN	NaN	NaN	NaN	NaN	NaN
UAN900027	1990.127	1990	2	16	7.786	0.145	7.786	0.145	4	NaN	NaN	NaN	NaN	NaN	NaN
UAN900048	1990.315	1990	4	26	7.932	0.112	7.969	0.06	5	7.894	0.164	3	NaN	NaN	3
UAN910361	1991.658	1991	8	29	8.695	0.06	8.775	0.057	3	8.592	0.09	3	8.718	0.032	3
UAN920469	1992.211	1992	3	18	9.012	0.025	9.012	0.025	3	NaN	NaN	NaN	NaN	NaN	NaN
UAN920655	1992.727	1992	9	23	9.152	0.049	9.18	0.042	4	9.135	0.059	5	9.14	0.046	3
UAN930279	1993.164	1993	3	2	9.321	0.023	9.353	0.024	3	NaN	NaN	NaN	9.289	0.023	3
UAN940378	1994.112	1994	2	11	10.205	0.054	10.291	0.077	3	10.17	0.072	3	10.154	0.012	3
UAN940679	1994.318	1994	4	27	10.06	0.043	10.06	0.043	3	NaN	NaN	NaN	NaN	NaN	NaN
UAN941096	1994.759	1994	10	4	10.259	0.192	10.259	0.192	4	NaN	NaN	NaN	NaN	NaN	NaN
UAN950527	1995.195	1995	3	13	10.596	0.023	10.596	0.023	4	NaN	NaN	NaN	NaN	NaN	NaN
UAN950789	1995.447	1995	6	13	10.788	0.059	10.82	0.088	6	NaN	NaN	NaN	10.756	0.03	3
UAN950894	1995.584	1995	8	2	11.202	0.157	11.202	0.157	4	NaN	NaN	NaN	NaN	NaN	NaN
UAN960115	1995.811	1995	10	24	11.027	0.109	11.027	0.109	4	NaN	NaN	NaN	NaN	NaN	NaN
UAN960051	1995.923	1995	12	4	11.081	0.052	11.108	0.06	3	11.054	0.044	5	NaN	NaN	NaN
UAN960957	1996.404	1996	5	28	11.39	0.056	11.407	0.068	5	NaN	NaN	NaN	11.373	0.043	3

UAN961164	1996.637	1996	8	21	11.705	0.123	11.705	0.123	3	NaN	NaN	NaN	NaN	NaN	NaN
UAN961409	1996.754	1996	10	3	11.668	0.04	11.695	0.074	3	NaN	NaN	NaN	11.64	0.006	3
UAN970092	1996.885	1996	11	20	11.728	0.044	11.766	0.069	4	11.726	0.031	4	11.693	0.033	3
UAN970008	1997.016	1997	1	7	11.809	0.06	11.871	0.114	5	11.767	0.051	5	11.79	0.016	3
UAN970011	1997.016	1997	1	7	11.813	0.081	11.824	0.123	3	NaN	NaN	NaN	11.802	0.039	3
UAN970010	1997.017	1997	1	7	11.812	0.062	11.812	0.062	3	NaN	NaN	NaN	NaN	NaN	NaN
UAN970380	1997.195	1997	3	13	11.934	0.063	11.97	0.085	13	NaN	NaN	NaN	11.898	0.041	6
UAN970754	1997.255	1997	4	4	12.245	0.071	12.245	0.071	4	NaN	NaN	NaN	NaN	NaN	NaN
UAN970756	1997.408	1997	5	30	12.194	0.046	12.3	0.093	5	12.17	0.019	4	12.112	0.027	3
UAN971115	1997.534	1997	7	15	12.263	0.057	12.281	0.044	3	12.244	0.07	7	NaN	NaN	NaN
UAN980724	1998.285	1998	4	15	12.902	0.116	12.902	0.116	5	NaN	NaN	NaN	NaN	NaN	NaN
UAN980918	1998.479	1998	6	25	13.052	0.081	13.051	0.086	6	13.053	0.077	5	NaN	NaN	NaN
UAN981563	1998.786	1998	10	15	13.25	0.062	13.323	0.091	15	NaN	NaN	NaN	13.177	0.032	3
UAN991060	1999.129	1999	2	17	13.606	0.089	13.606	0.089	6	NaN	NaN	NaN	NaN	NaN	NaN
UAN991062	1999.279	1999	4	13	13.717	0.067	13.737	0.026	4	13.696	0.108	5	NaN	NaN	NaN
UAN991381	1999.59	1999	8	4	13.904	0.088	13.904	0.088	3	NaN	NaN	NaN	NaN	NaN	NaN
UAN992045	1999.874	1999	11	16	14.152	0.11	14.152	0.11	5	NaN	NaN	NaN	NaN	NaN	NaN
UAN20101335	2000.164	2000	3	1	14.375	0.088	NaN	NaN	NaN	14.375	0.088	6	NaN	NaN	NaN
UAN992982	2000.199	2000	3	14	14.391	0.092	14.393	0.139	6	14.426	0.111	5	14.353	0.028	3
UAN993562	2000.744	2000	9	29	14.818	0.044	14.818	0.044	4	NaN	NaN	NaN	NaN	NaN	NaN
UAN993563	2001.038	2001	1	15	14.979	0.089	15.002	0.111	7	14.977	0.133	4	14.957	0.022	3

UAN994885	2001.545	2001	7	19	15.534	0.104	15.53	0.116	3	15.539	0.093	5	NaN	NaN	NaN
UAN994886	2002.466	2002	6	20	16.11	0.075	16.08	0.105	4	16.13	0.086	6	16.121	0.035	3
UAN995445	2003.129	2003	2	17	16.54	0.071	16.596	0.08	6	16.481	0.079	5	16.544	0.053	3
UAN996454	2003.384	2003	5	21	16.802	0.071	16.802	0.071	3	NaN	NaN	NaN	NaN	NaN	NaN
UAN996455	2003.753	2003	10	3	17.018	0.062	17.081	0.096	4	16.967	0.057	5	17.005	0.032	3
UAN996456	2004.053	2004	1	20	17.265	0.113	17.265	0.113	3	NaN	NaN	NaN	NaN	NaN	NaN
UAN998318	2004.057	2004	1	22	17.237	0.058	17.275	0.072	5	17.24	0.059	6	17.195	0.042	3
UAN996457	2004.268	2004	4	8	17.523	0.205	17.523	0.205	3	NaN	NaN	NaN	NaN	NaN	NaN
UAN996458	2004.459	2004	6	17	17.529	0.025	17.53	0.026	3	NaN	NaN	NaN	17.529	0.025	3
UAN997089	2004.915	2004	12	1	17.879	0.075	17.932	0.075	16	17.826	0.075	18	NaN	NaN	NaN
UAN997090	2005.11	2005	2	10	18.009	0.037	17.991	0.052	5	18.028	0.021	5	NaN	NaN	NaN
UAN998005	2005.488	2005	6	28	18.36	0.098	18.345	0.175	14	18.413	0.095	18	18.32	0.025	6
UAN998006	2005.759	2005	10	5	18.653	0.122	18.653	0.122	8	NaN	NaN	NaN	NaN	NaN	NaN
UAN998195	2006.11	2006	2	10	18.873	0.134	18.905	0.204	14	18.853	0.173	15	18.862	0.025	6
G-139	2006.756	2006	10	4	19.695	0.12	NaN	NaN	NaN	19.695	0.12	6	NaN	NaN	NaN
UAN998425	2006.797	2006	10	19	19.65	0.042	NaN	NaN	NaN	19.696	0.043	6	19.603	0.042	4
UAN998852	2006.942	2006	12	11	19.784	0.094	19.778	0.134	5	19.791	0.054	4	NaN	NaN	NaN
UAN998898	2007.348	2007	5	8	20.132	0.098	NaN	NaN	NaN	20.132	0.098	5	NaN	NaN	NaN
UAN999276	2007.89	2007	11	22	20.733	0.181	NaN	NaN	NaN	20.726	0.308	5	20.741	0.054	3
UAN999627	2008.347	2008	5	7	21.198	0.014	NaN	NaN	NaN	NaN	NaN	NaN	21.198	0.014	3
UAN999756	2008.612	2008	8	12	21.365	0.067	NaN	NaN	NaN	21.364	0.086	6	21.365	0.049	3

UAN20100047	2008.956	2008	12	16	21.773	0.071	NaN	NaN	NaN	21.773	0.071	5	NaN	NaN	NaN
UAN20100609	2009.175	2009	3	6	21.836	0.09	NaN	NaN	NaN	21.851	0.118	8	21.821	0.062	3
UAN20101456	2009.567	2009	7	27	22.051	0.031	NaN	NaN	NaN	NaN	NaN	NaN	22.051	0.031	3

Supplementary Material (3): Emissions Inventories

HFC-23 (trifluoromethane, fluoroform, CHF_3) is a by-product of the chemical process to manufacture HCFC-22 (chlorodifluoromethane, $CHClF_2$) from chloroform and hydrogen fluoride.

S3.1. HCFC-22 Production

HCFC-22 is used in two ways: the commercial product is used in the refrigeration and air conditioning industries, and is eventually emitted into the atmosphere; production and consumption for this are controlled under the Montreal Protocol . It is also a chemical feedstock, the raw material for the manufacture of PTFE (polytetrafluoroethylene) and other fluoropolymers, effectively being destroyed in the process with small, inadvertent emissions not controlled under the Montreal Protocol.

Table S3 shows the inventory of HCFC-22 production for all end uses, subdivided between developed countries (referred to in the Montreal Protocol as "non-Article 5 countries", that are not eligible for any support under the Montreal Protocol or United Nations Framework Convention on Climate Change (UNFCCC) mechanisms, and individual Article 5 countries that are eligible to receive support to reduce emissions of HFC-23.

In the case of the non-A5 countries (which are listed individually in Table S4), historical demand for dispersive uses was taken from the AFEAS database [(1)] up to 2007 and demand for fluoropolymer feedstock was derived from Stanford Research Institute data [(2)] that shows historical linear growth at 5800 tonnes/year from 2001 onwards and a requirement of about 50% of the reported dispersive demand up to that date. Production for dispersive use in 2008 was derived from the Parties submissions to the Montreal Protocol [(3)] and the Technology and Economic Assessment Panel of the Montreal Protocol [(4)]. From 2009 onwards, the total production reported to the Executive Committee of the Montreal Protocol was used [(5)].

The same report to the Executive Committee [(5)] was used for production from individual Article 5 countries from 2009 onwards; prior to that year, the quantities produced in Argentina, India, South Korea, Mexico and Venezuela were estimated using the Montreal Protocol and TEAP data [(3, 4)].

Table S3. Estimated HCFC-22 production: Total for all uses Gg.

Year	Non-Article 5 Countries	Article 5 Countries						Global Total
		Argentina	China	India	Korea (N)	Korea (S)	Mexico	Venezuela	
1990	320.57	0	0	3.62	0	1.75	1.54	1.85	329.33
1990	320.57	0	0	3.62	0	1.75	1.54	1.85	329.33
1991	355.22	0	0	3.86	0	2.65	1.84	1.80	365.37
1992	368.57	0	0	3.72	0	3.97	1.86	2.04	380.16
1993	360.93	0.18	4.92	4.72	0	4.41	2.82	2.01	379.99
1994	359.17	0.21	9.83	4.50	0	4.51	2.14	1.43	381.79
1995	365.20	0.00	14.75	5.22	0	5.09	1.96	1.45	393.67
1996	406.86	0.00	19.66	4.54	0	8.27	4.80	1.39	445.53
1997	376.66	0.00	24.58	5.33	0	9.28	4.67	1.37	421.89
1998	391.76	0.00	37.14	8.34	0	7.88	3.42	0.95	449.48
1999	378.56	0.00	59.74	8.68	0	14.42	4.89	1.07	467.37
2000	365.77	0.11	77.79	11.18	0	11.29	3.43	1.20	470.77
2001	345.20	0.11	111.42	12.01	0	5.81	2.59	1.32	478.46
2002	331.76	0.58	103.37	11.26	0	10.22	3.81	1.44	462.44
2003	326.63	1.06	144.22	13.88	0	6.84	3.70	1.57	497.89
2004	334.73	1.54	191.06	17.99	0	5.53	3.73	1.69	556.26
2005	327.37	2.01	270.89	17.41	0	7.92	5.53	1.81	632.93
2006	322.29	2.49	325.28	21.06	0	5.23	7.33	1.94	685.61
2007	328.10	2.96	414.97	29.32	0	4.94	9.13	2.06	791.47
2008	333.92	3.44	373.17	38.49	0	5.93	10.93	2.18	768.05
2009	195.80	3.91	483.98	47.66	0.50	6.91	12.73	2.31	753.80
2010	229.86	4.25	549.27	47.61	0.50	7.63	12.62	2.17	853.91
2011	241.78	4.02	596.98	48.48	0.48	7.26	11.81	2.44	913.26
2012	219.91	4.19	644.49	48.18	0.52	5.70	7.87	2.91	933.77
2013	193.52	1.95	615.90	40.65	0.58	6.67	7.38	2.20	868.86
2014	210.04	2.29	623.90	54.94	0.53	6.83	9.21	1.57	909.30
2015	225.16	2.45	534.93	53.31	0.50	7.18	4.75	0.68	828.95

Chinese production now accounts for 65% of the global total, with a large demand for fluoropolymer feedstock, and was estimated separately. Production for dispersive uses and export was derived from the submission to the Montreal Protocol database and TEAP data [3, 4]. Fluoropolymer (mainly polytetrafluoroethylene, PTFE) production from 1998 to 2002 was reported in China Chemical Reporter (CCR) [6] and showed growth of 33%/year. This growth was assumed to be maintained until 2007, implying production of over 69 Gg/year of PTFE in 2007, a value consistent with the capacity for fluoropolymers stated in the 11th Chinese 5 year plan to be 80 Gg/year in 2007/8 [7]. Total production of HCFC-22 in China was also reported in CCR [6], with a growth rate of between 47% and 25% in the period 1998 to 2001. For the values calculated here, a subsequent growth rate of 15% / year was applied until 2008, and from 2009 onwards, the total annual productions reported to the Executive Committee of the Montreal Protocol were used [5].The resulting values agree within 4% with the numbers for 2013 to 2015 reported separately by the Chinese government [8].

S3.2. HFC-23 Emissions

Attempts to reduce HFC-23 formation by adjusting process conditions have important economic consequences for HCFC-22 production; the historic rate of HFC-23 production from a plant optimised for HCFC-22 production is 4% [9]. In plants, constructed in the last 10 years, this has been reduced to about 3% [5]. HFC-23 has few uses, some of which (for example, as a fire suppressing agent) will result in the eventual emission of most or all into the atmosphere. In the 21st century emissions from these uses have been almost constant at 133 ± 9 metric tonnes year^{-1}, a maximum of 10% of all emissions [10]. Prevention of emissions of HFC-23 requires the capture and treatment of the process vent stream, generally accomplished by high temperature oxidation.

Developed country signatories to the United Nations Framework Convention on Climate Change (UNFCCC), essentially the same set as the non-A5 countries, are required to report emissions of each HFC greenhouse gas each year. The emissions reported by individual countries are shown in the first columns of Table S4 [10]; changes in accounting procedure, such as happened in Germany from 2007 were accommodated by using the original contemporaneous data files (rather than the compendia published in 2017). This is consistent with the step changes, that resulted either from closure of the HCFC-22 production facility or from capture and thermal oxidation of the HFC-23, and with pollutant reports to national authorities [11, 12].

The second set of columns in Table S4 shows the estimated emissions of HFC-23 from those countries that are eligible for assistance under the Clean Development Mechanism (CDM) of the UNFCCC. Essentially, this rewarded destruction of HFC-23 at 11700 times the value of the same mass of CO_2, a gearing ratio that distorted the economics of HCFC-22 production [13] and led to the closure of the CDM to HFC-23 projects after 2009. The decision of the EU to ban the use of HFC-23 certified emission reduction (CER) credits in the European Union Emissions Trading System from 1 May 2013 effectively rendered these CERs valueless [5].

The emissions in Table S4 were calculated by estimating the annual production of HFC-23 for each country and then subtracting the quantity estimated to have been abated.

Argentina and Mexico - from 1990 to 2011, production of HFC-23 was estimated at 3.6%, falling to 3% of HCFC-22 production; from 2012 to 2015, the actual productions reported by the Executive Committee of the Montreal Protocol [5] were used. This was abated up to the maximum claimed under the CDM [14] up to May 2013, after which the destruction facilities were apparently shut down and the HFC-23 was released into the atmosphere [5].

China - from 1990 to 2006, a production rate of 3.6% was assumed, falling to 2.8% subsequently[5]. Abatement at the maximum rate allowed for the 11 of 32 plants operating under the CDM was then assumed until 2012 with the other 21 plants operating without abatement. From 2012 onwards, the actual emissions reported by China were used [5]. The quantities of HFC-23 destroyed in the period 2007 to 2015 varied between 28 and 47% of that produced.

India - up to year 2000, a production rate of 3.6% was assumed, which then dropped to 2.9%. Apparently, all of the India plants have abatement technology and, after 2006, no emissions were estimated.

South Korea - a production rate of 4%, falling to 3% was assumed for the period 1990 to 2008. Subsequently the production reported to the Executive Committee was used [5]. This was abated at the maximum allowed within the CDM until 2012, when the destruction facility was shut down. Although the HFC-23 is recovered for sale, much of that will be emitted and this is reflected in the values shown for South Korea.

North Korea - there are no data prior to 2009 and defaults of zero have been used. From 2009 onwards, the estimates here are those given in Reference 5, with total emission.

Venezuela - the production rate throughout is set at 3%, with no abatement.

1

Table S4. National HFC-23 Emissions (Metric tonnes Mt or Mg)

Year	Countries Reporting to UNFCCC under CRF												Countries Reporting Data under CDM							Total Annual Emission Gg
	Australia	Canada	France	Germany	Greece	Italy	Japan	Netherlands	Russia	Spain	UK	USA	Argentina	China	India	Korea (N)	Korea (S)	Mexico	Venezuela	
1990	48.1	65.6	142.0	373.4	79.9	30.0	717.6	378.8	2428.2	205.4	972.3	3127.6	0.0	0.0	130.4	0.0	70.0	55.5	55.4	8.88
1991	96.3	71.4	184.6	342.9	94.6	30.0	1140.3	295.0	2312.8	186.2	1012.3	2812.0	0.0	0.0	138.9	0.0	106.1	66.1	54.0	8.94
1992	93.2	56.1	173.7	342.4	77.6	30.0	1185.7	378.0	1904.6	236.1	1052.4	3123.9	0.0	0.0	134.0	0.0	158.6	67.1	61.2	9.07
1993	106.9	0.0	177.5	342.1	137.3	30.0	1173.0	424.2	1234.3	193.0	1092.4	2846.9	5.4	176.9	170.0	0.0	176.4	101.4	60.4	8.45
1994	96.5	0.0	79.4	342.6	183.2	30.0	1248.8	544.2	1044.1	295.5	1132.5	2716.1	6.3	353.9	162.1	0.0	180.4	77.0	42.8	8.54
1995	65.4	0.1	19.5	302.8	278.0	30.8	1432.0	503.0	1042.3	396.5	1192.6	2843.7	0.0	530.8	187.9	0.0	223.1	70.4	43.5	9.16
1996	30.7	0.1	32.9	263.6	320.2	1.2	1422.3	611.9	917.5	432.4	1220.7	2690.9	0.0	707.8	163.4	0.0	330.9	172.9	41.7	9.36
1997	0.0	0.9	31.6	254.7	338.9	1.6	1328.5	621.8	1212.3	495.9	1330.8	2601.3	0.0	884.7	192.0	0.0	278.3	168.0	41.1	9.78
1998	0.0	0.3	20.6	246.5	373.6	2.5	1245.3	711.3	1468.2	437.1	1030.2	3411.2	0.0	1337.0	300.2	0.0	166.1	122.9	28.5	10.90
1999	0.1	0.4	38.7	233.5	430.9	2.5	1233.2	318.5	1523.2	511.5	409.9	2636.6	0.0	2175.8	312.6	0.0	311.2	176.2	32.2	10.35
2000	0.1	0.5	31.9	109.1	321.7	3.0	1149.7	223.8	1783.7	557.2	219.1	2468.6	3.4	2827.1	402.6	0.0	276.7	123.4	35.9	10.54
2001	0.1	0.5	33.0	99.6	275.1	3.4	933.7	41.9	1680.8	270.0	196.8	1702.6	3.2	4036.4	353.0	0.0	47.6	93.1	39.6	9.81
2002	0.1	0.5	34.2	110.1	277.2	3.9	667.1	62.4	1268.3	120.4	165.4	1819.0	17.5	3780.5	330.9	0.0	145.0	137.3	43.3	8.98
2003	0.1	0.6	23.4	53.8	232.8	4.6	527.7	37.8	933.5	176.0	158.9	1066.3	31.8	5274.9	408.0	0.0	145.2	133.0	47.0	9.26
2004	0.2	0.6	30.3	53.2	224.1	5.3	261.6	31.9	1160.8	98.8	29.4	1488.3	46.1	6945.8	365.0	0.0	46.0	134.3	50.7	10.97
2005	0.2	0.6	35.4	53.8	191.4	6.0	85.5	17.6	1217.7	92.2	28.0	1368.9	60.3	9916.5	50.1	0.0	117.5	199.0	54.4	13.50
2006	0.2	0.6	42.3	35.9	7.7	6.7	90.3	25.0	1045.8	109.4	17.2	1201.1	74.6	11132.2	0.0	0.0	37.0	0.0	58.1	13.88
2007	0.3	0.6	26.8	10.6	11.6	7.5	63.8	21.8	943.0	98.8	8.3	1470.0	0.0	7872.6	0.0	0.0	28.1	33.5	61.8	10.66
2008	0.3	0.6	29.0	9.5	12.6	8.3	71.5	19.2	955.9	101.7	4.7	1180.3	0.0	5726.7	0.0	0.0	57.8	82.7	65.5	8.33
2009	0.3	0.5	15.2	8.2	12.9	8.4	36.7	13.8	571.9	90.9	3.8	473.3	0.0	7848.3	0.0	9.1	87.4	126.6	69.2	9.38
2010	0.3	0.6	11.6	7.8	15.0	9.0	9.6	34.9	572.8	122.9	1.1	559.1	0.0	9165.0	0.0	9.0	109.0	124.0	65.0	10.82
2011	0.4	0.7	7.5	8.3	13.3	9.3	6.1	15.0	317.1	78.2	1.0	607.9	0.0	9961.3	0.0	8.6	97.9	104.4	73.3	11.31
2012	0.4	0.7	8.0	7.8	14.9	9.2	4.3	11.3	637.1	69.9	0.9	386.2	0.0	10753.9	0.0	8.4	51.1	8.1	87.4	12.06
2013	0.4	0.7	9.1	7.4	15.1	9.4	4.3	17.5	798.7	60.6	1.0	290.1	29.3	10841.1	0.0	10.6	100.1	88.0	66.1	12.35
2014	0.5	0.6	9.2	7.2	12.2	9.6	5.2	3.9	912.2	55.7	1.2	364.2	68.6	12492.5	0.0	7.8	205.0	202.8	47.0	14.41
2015	0.5	0.6	9.3	6.7	11.9	9.8	6.7	9.1	665.6	46.4	1.4	313.0	73.4	7481.8	0.0	7.4	204.0	100.8	20.3	8.97

Notes.

[1] Production of HCFC-22 up to 2007 in non-Article 5 countries downloadable from *https://agage.mit.edu/data/agage-data*

[2] Stanford Research Institute, International, 1998: Fluorocarbons, Sections 543.7001 to 543.7005 of *Chemical Economics Handbook*, SRI International, Menlo Park, USA, updated using Will R. and H. Mori, Fluorocarbons, Chemical Economics Handbook 543.7000 of SRI Consulting, Access Intelligence (*www.sriconsulting.com*), 2008.

[3] Production and Consumption of Ozone Depleting Substances under the Montreal Protocol, 1986-2015, *United Nations Environment Programme*, available at *http://ozone.unep.org/en/data-reporting/data-centre*

[4]UNEP 2006 Assessment Report of the Technology and Economic Assessment Panel, *United Nations Environment Programme*, Nairobi, 2006.

[5] Key aspects related to HFC-23 by-product control technologies (Decision 78/5), Report to the Executive Committee of the Multilateral Fund for the Implementation of the Montreal Protocol, UNEP/OzL.Pro/ExCom/79/48 of 7 June 2017 available at *ozone.unep.org*

[6] Market Report: Fluorochemical develops rapidly in China, *China Chemical Reporter, 13*, Sep 6, 2002.

[7] Development and Forecast Report on China Fluorine Industry between 2007 and 2008, *www.acunion.net*, 2009.

[8] Wang Kaixiang, HCFCs/HFCs Production in China, Foreign Economic Cooperation Office, FECO/MEP, May 2015.

[9] Intergovernmental Panel on Climate Change. Revised 1996 Guidelines for National Greenhouse Gas Inventories, Reference manual, vol 3, *IPCC/IGES*, Kanagawa, Japan, 1996.

[10] Data reported under the *Common Reporting Format* and in *National Inventory Reports* available at *http://unfccc.int/national_reports/annex_i_ghg_inventories/ national_inventories_submissions/items/10116.php*.

[11] US EPA Facility Level Greenhouse Gas Emissions Data available at *https://ghgdata.epa.gov/ghgp/main.do*

[12] European Pollutant Release and Transfer Register (E-PRTR) available at *http://prtr.ec.europa.eu*

[13]Munnings C., B. Leard and A. Bento, The net emissions impact of HFC-23 offset projects from the Clean Development Mechanism, Resources for the Future, Discussion Paper 16-01, 2016.

[14] UNFCCC, Clean Development Mechanism Project Activities available at *http://cdm.unfccc.int/Projects/Index.html*

Supplementary Material (4): Influence of OH on the inversions.

Small differences were found in the derived emissions of HCFC-22, whereas, owing to its very long lifetime, negligible differences were found for HFC-23.

For HCFC-22, the magnitude of the difference when Rigby et al., (2017) OH was used versus an annually repeating OH concentration was much smaller than the derived uncertainty.

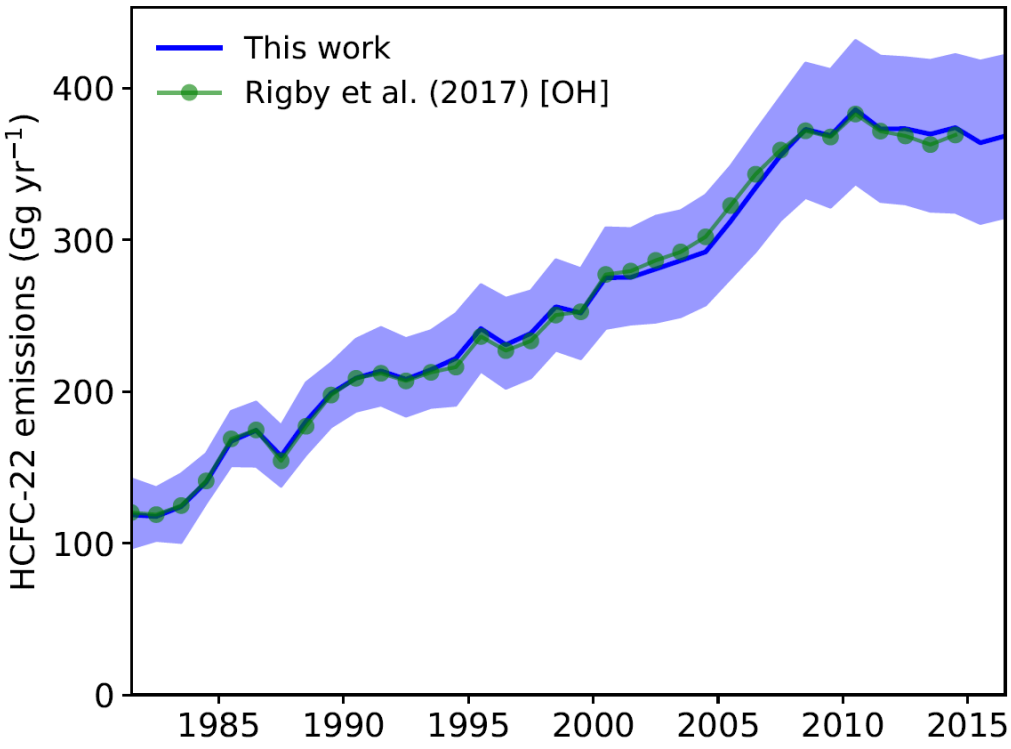

Figure S3. Potential variations in OH concentrations on the inversions

Supplementary Material (5): European Estimates Using FLEXPART and Empa Inversion

Detailed Results

The inversion results suggest that European emissions of HFC-23 in general were larger than reported to UNFCCC and exhibited considerable year-to-year variability. *A posteriori* estimates from the two inversions using different *a priori* emissions mostly agree with each other within the scope of their uncertainty limits (see Figure 6 in the main manuscript and Figure S4). Exceptions are the Italian estimates for the years 2013 and 2015, when the use of the UNFCCC a-priori resulted in much larger *a posteriori* emissions than the use of the 'UNFCCC r0.5' *a priori*. Furthermore, a large difference was also obtained for France in 2013, again the UNFCCC inversion yielding larger *a posteriori* emissions than the UNFCCCC r0.5 inversion. All regions except Spain exhibited larger *a posteriori* than *a priori* emissions for all years. These differences were most significant for Italy where average *a posteriori* emissions of 38±10 Mg/yr were estimated for the years 2009 to 2016. Although Italian *a posteriori* emissions were relatively low and closer to the *a priori* estimate in 2016 there is no clear negative trend in the emissions. Emissions from the Benelux region grew steadily until 2013 and dropped sharply afterwards, a tendency only partly reflected in the UNFCCC estimates. French *a posteriori* emissions agreed fairly well with the UNFCCC reports, with the exception of 2013 when at least one of the inversions yielded significantly higher emissions. A similar statement can be made for the United Kingdom, where only the *a posteriori* estimates for the year 2014 deviates more strongly form the UNFCCC values. The German *a posteriori* emissions were considerably larger than the *a priori* until 2012, thereafter they were closer to the reported UNFCCC values. Our *a posteriori* estimates for the Iberian Peninsula remained relatively close to the UNFCCC *a priori*. Total emissions for the six European regions listed in Table 4 (main manuscript) ranged from 108±30 Mg/yr in 2015 up to 293±43 Mg/yr in 2013 and showed a slightly negative, but insignificant trend for the period analysed here.

Compared to previous estimates by Keller et al. (2011) the estimates in this study for the years 2009 and 2010 are similar for Italy and the Benelux region, but were considerably smaller for Germany, France and the UK. The large difference for Germany may be explained by the much larger *a priori* estimate of 50 Mg/yr in Keller et al. (2011). For France and the UK similar *a priori* values were used and the differences may result from different selection of observation data. In Keller et al. (2011) the inversion was done for observations from July 2008 to July 2010, whereas here each inversion is based on one calendar year of observations.

The model performance was analysed at both Jungfraujoch and Mace Head with respect to correlations and root mean square error of simulated versus simulated time series (Figure S5). A large part of the correlation between simulation and observation is actually due to the increasing trend in HFC-23. Therefore, the correlation of the above-baseline signal can be seen as a better metric for the model performance. The latter increased considerably from a-priori to *a posteriori* for Jungfraujoch and only slightly for Mace Head. Again, there was

year-to-year variability in the correlation coefficient and for Jungfraujoch a tendency to smaller correlation coefficients for later years can be seen.

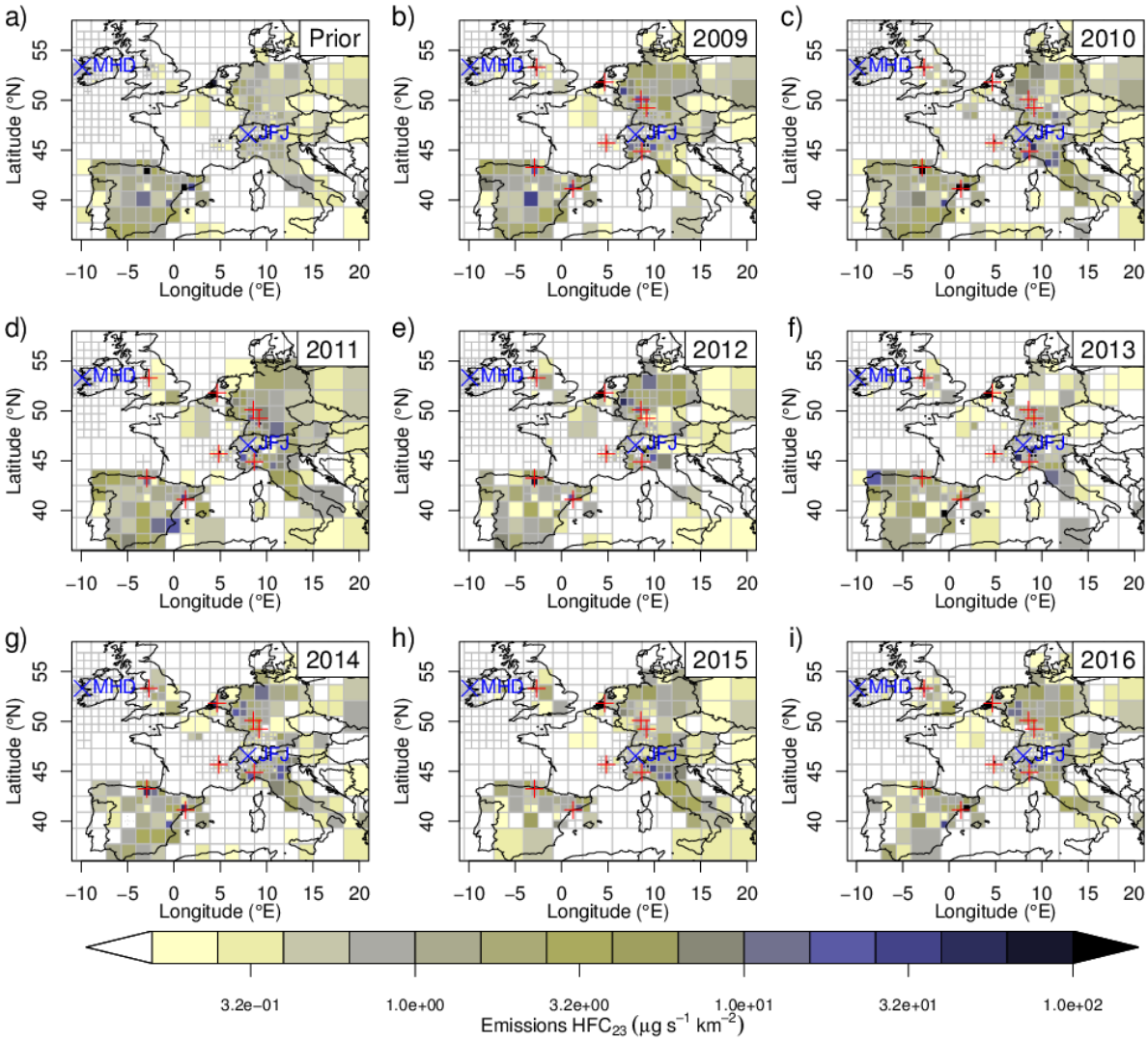

Figure S4: Spatial distribution of HFC-23 *a posteriori* emissions (b-i) as estimated when using the UNFCCC *a priori* emissions (a). Red crosses mark the location of past and present HCFC-22 production plants.

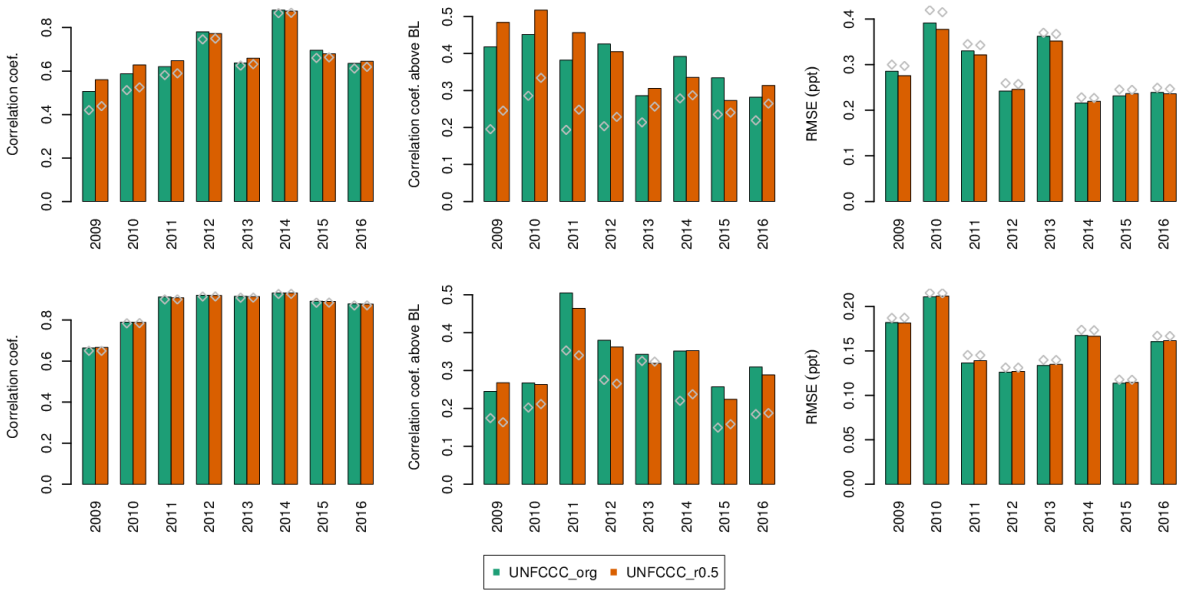

Figure S5: Regional scale transport model skills as evaluated against Jungfraujoch (top) and Mace Head (bottom) observations. *A priori* performance is shown as shaded bars and *a posteriori* performance as solid bars. (left) correlation coefficient for the complete time series, (centre) correlation coefficient for the regional (above baseline) part of the time series, (right) root mean square error.

References

Brunner, D., Arnold, T., Henne, S., Manning, A., Thompson, R. L., Maione, M., O'Doherty, S., and Reimann, S.: Comparison of four inverse modelling systems applied to the estimation of HFC-125, HFC-134a and SF_6 emissions over Europe, Atmos. Chem. Phys. Discuss., 2017, 1-29, 2017.

Gridded Population of the World, Version 4 (GPWv4): Population Density Adjusted to Match 2015 Revision UN WPP Country Totals: http://dx.doi.org/10.7927/H4HX19NJ, 2016.
Henne, S., Brunner, D., Oney, B., Leuenberger, M., Eugster, W., Bamberger, I., Meinhardt, F., Steinbacher, M., and Emmenegger, L.: Validation of the Swiss methane emission inventory by atmospheric observations and inverse modelling, Atmos. Chem. Phys., 16, 3683-3710, doi: 10.5194/acp-16-3683-2016, 2016.

Keller, C. A., Brunner, D., Henne, S., Vollmer, M. K., O'Doherty, S., and Reimann, S.: Evidence for under-reported western European emissions of the potent greenhouse gas HFC-23, Geophys. Res. Lett., 38, L15808, doi: 10.1029/2011GL047976, 2011.

Seibert, P., and Frank, A.: Source-receptor matrix calculation with a Lagrangian particle dispersion model in backward mode, Atmos. Chem. Phys., 4, 51-63, doi: 10.5194/acp-4-51-2004, 2004.

Stohl, A., Forster, C., Frank, A., Seibert, P., and Wotawa, G.: Technical note: The Lagrangian particle dispersion model FLEXPART version 6.2, Atmos. Chem. Phys., 5, 2461-2474, doi: 10.5194/acp-5-2461-2005, 2005.

Supplementary Material (6): Additional HFC-23 emissions

Table S5. Annual mean global HFC-23 (CHF_3) emissions derived from the AGAGE 12-box model.

Year	HFC-23 Global annual emissions (Gg yr^{-1}) ±1 sigma (σ) SD.	Year	HFC-23 Global annual emissions (Gg yr^{-1}) ±1 sigma (σ) SD.
1930	0.54 ± 2.0	1955	0.11 ± 1.4
1931	0.52 ± 1.4	1956	0.16 ± 1.4
1932	0.50 ± 1.3	1957	0.20 ± 1.4
1933	0.47 ± 1.3	1958	0.29 ± 1.3
1934	0.44 ± 1.1	1959	0.39 ± 1.3
1935	0.41 ± 1.1	1960	0.43 ± 1.4
1936	0.37 ± 1.2	1961	0.50 ± 1.4
1937	0.34 ± 1.2	1962	0.62 ± 1.4
1938	0.30 ± 1.3	1963	0.76 ± 1.3
1939	0.27 ± 1.3	1964	0.92 ± 1.3
1940	0.24 ± 1.3	1965	1.10 ± 1.4
1941	0.20 ± 1.4	1966	1.33 ± 1.4
1942	0.17 ± 1.3	1967	1.60 ± 1.4
1943	0.15 ± 1.4	1968	1.94 ± 1.2
1944	0.12 ± 1.3	1969	2.15 ± 1.4
1945	0.09 ± 1.5	1970	2.24 ± 1.3
1946	0.07 ± 1.3	1971	2.38 ± 1.2
1947	0.05 ± 1.3	1972	2.61 ± 1.2
1948	0.04 ± 1.2	1973	2.95 ± 1.2
1949	0.03 ± 1.3	1974	2.98 ± 1.2
1950	0.02 ± 1.2	1975	2.99 ± 1.2
1951	0.01 ± 1.2	1976	2.95 ± 1.0
1952	0.02 ± 1.5	1977	3.17 ± 1.0
1953	0.04 ± 1.2	1978	3.62 ± 1.0
1954	0.06 ± 1.3	1979	3.92 ± 0.8

We thank the Referee #1 for their time and effort in evaluating this manuscript and for their suggestions for improvements. Our responses to the points made by the reviewer are addressed on the following pages.

Replies to Referee 1

1 Overview:

Review of "Recent increases in the growth rate and emissions of HFC-23 (CHF3) and the link to HCFC-22 (CHClF2) production" by Simmonds et al.
Simmonds et al. present an estimate of the HFC-23 and HCFC-22 emissions using observations from the AGAGE network. They perform two Bayesian inversions: (1) in a global 12-box model and (2) a regional inversion for Europe using FLEXPART. Overall, the manuscript reaches scientifically interesting conclusions. However, many of the details necessary to follow the conclusions are not included. Specifically, most of the details of the forward and inverse modelling are omitted. This makes it difficult to interpret the results. Additionally, some of the conclusions seem overly speculative.

I would suggest major revisions for the manuscript.

2 Major comments:

2.1 Structure of the manuscript and description of the modelling
The authors spend most of the methods section explaining the measurement protocols and calibration methods. Are the measurements used here fundamentally different from the previous work using the same AGAGE measurements? It seems that this paper is, at it's core, an inverse modelling paper because the novel analysis is related to the derived emissions. However, the forward and inverse modelling is not well described. The authors spend a single paragraph explaining the 12-box model. Is the box-model including a seasonal cycle or annual concentrations? If there is not a seasonal cycle, how are the authors removing the seasonal cycle from the observations? The authors mention that they use an inter-annually repeating OH but some recent work (Rigby et al., PNAS, 2017; Turner et al., PNAS, 2017) has shown variations in OH, would this be important for the modelling here?

Reply. We have added further detail to Section 2.6 to provide further details on the inverse method. Similarly to the reviewer's concerns regarding the length of the description of the measurements, we opted to keep this section brief, because the methods have been described in detail elsewhere (Rigby et al., 2011; Rigby et al., 2013; Rigby et al; 2014). Regarding the influence of OH variations on the inversion, small differences were found in the derived emissions of HCFC-22 (which we now show in the supplement), whereas, owing to its very long lifetime, negligible differences were found for HFC-23. For HCFC-22, the magnitude of the difference when Rigby et al (2017) OH was used versus a constant OH concentration were much smaller than the derived uncertainty (Supplementary Information).

Questions related to the 12-box model inversion: How is the inversion done? What is the state vector? Is it annual global emissions or the emissions for each of the latitudinal boxes? Presumably the distributions are Gaussian? Are there off-diagonal covariances? How are the model-data uncertainties specified (ie., what is the model error)? Some of these details could go in a supplement, but they should be described somewhere.

Reply. We have added this information to Section 2.6.

Similarly, the authors present a second inverse analysis within the results section (Section 3.2). The modelling is explained in a single paragraph, yet this is a very complicated inverse model they present. In the paragraph that follows, the authors state "Considerable differences between the two inversions with different a priori emission distributions occurred on the country scale" but do not explain the different inversions, priors, etc. Supplemental Section 3 provides a good explanation of the inversion framework from Brunner and Henne and I would recommend incorporating some of that text in the manuscript, it would be very useful for the reader.

Reply. We agree with the referee that more details of the regional inversion could have been included in the main text. However, it was the intention to keep the text as concise as possible and the applied inversion tool has frequently been used in previous studies. Nevertheless, we follow the suggestion of the referee and included the details on the inversion method in a new section (3.7) in the main text, while keeping the more comprehensive discussion of the inversion results in the supplementing material.

2.2 Differences between this work and Miller et al., (2010)?
The authors note that "Miller et al., (2010) calculated global emissions of HCFC-23 using the same AGAGE 12-box model as used here, but with a different Bayesian inverse modelling framework." (Section 3.2). However, the authors do not seem to explain the differences between the inverse modelling frameworks. This seems like a crucial detail because the HFC-23 emissions from Miller et al. are outside the errorbars presented here (Figure 3). This comment seems to go back to my previous comment on the structure of the manuscript. The authors spent a lot of time explaining the measurements but, from my reading, it doesn't seem like the measurements are what give them different emissions.

Reply. It is important to note that the Miller et al (2010) emissions shown in Figure 3 are bottom-up estimates. We had omitted to specify this in the figure caption and have now added this in the revised version. Small differences are observed between the top-down estimates from Miller et al (2010) and those presented here. This is because: a) we include a new firn dataset in our inversion; b) Miller et al. (2010) constrained the inversion to absolute emissions from a time-varying prior, whereas we used a much simpler prior constraint that the assumed emissions growth rate would not vary by more than ±20% of the maximum bottom-up estimate, between any two years.

2.3 Speculative statements

There are a number of statements that seem overly speculative and it's not clear that they are supported by the analysis. Here I list two rather provocative statements:

Statement (Section 3.2): "We also note that this minimum occurred during the global financial crisis of 2007-2009 and in fact HFC-23 emissions mirror global GDP growth rates for the years before and after 2009https://data.worldbank.or/indicator.NY.GDP.MKTP.CD). We can only speculate that this may have reduced the overall demand for PTFE, thereby impacting global HCFC-22 production and the co-produced HFC-23."

Reply. This statement has been removed.

Statement (Conclusions): "With the support of the Chinese Government, 13 new destruction facilities at 15 HCFC-22 production lines not covered by CDM were started in 2014 (UNEP, (2017a). The timing of these new initiatives is consistent with the most recent reduction (2015-2016) of global HFC-23 emissions, although we cannot confirm a direct link."

Reply. Respectfully, we would wish to retain this statement of fact and have slightly edited the text as follows-:

In 2014, with the support of the Chinese Government, 13 new destruction facilities at 15 HCFC-22 production lines not covered by CDM were started (UNEP, (2017a). The time frame of these new initiatives is consistent with the most recent reduction (2015-2016) of global HFC-23 emissions.

We thank the Referee #2 for their time and effort in evaluating this manuscript and for their suggestions for improvements. Our responses to the points made by the reviewer are addressed on the following pages.

Replies to Referee 2

This manuscript reports an update of the evolution of global mole fractions and emissions of HFC-23, an important greenhouse gas. The findings are novel and interesting and the overall work is certainly of sufficient quality for publication in ACP. I would however suggest a) clarifying the reasons for publishing this gas separately from the 2017 Simmonds paper on HFCs and HCFCs and b) the following changes:

Reply. The principal reason for a separate paper on HFC-23 is that unlike the other HFCs this is not a replacement fluorocarbon, but a compound with a more unique history as an unavoidable by-product of HFC-22 production. As such, we felt that it deserved a separate analysis, consistent with increasing attention and interest from the atmospheric science community.

L33-36 I'm not sure what the authors want to say here. Does this mean that the HCFC22 production process has been releasing an increasingly high fraction of HFC-23 or are other sources important, too? This should be clarified in a concise way.

Reply. Here we are just reporting HCFC-22 mole fractions. The following sentence has been added to clarify.

This slowing growth is consistent with demand for HCFC-22 moving from dispersive to feedstock uses, but HFC-23 emissions are a consequence of incomplete mitigation from all HCFC-22 production.

L47-49 So which regions are likely to be responsible for the other 98.5 %?

Reply. We have added the following sentences.

The majority of the increase in global HFC-23 emissions is attributed to a delay in the adoption of mitigation technologies, predominately in China and East Asia. However, a reduction in emissions is anticipated, when the Kigali 2016 amendment to the Montreal Protocol requiring HCFC and HFC production facilities to introduce destruction of HFC-23 is fully implemented.

L53-58 This sentence is very long. Consider splitting it up to improve readability. L75 The date of that reference is inconsistent with the one in the reference list.

Reply. Sentence has been split into two as requested. We also thank the referee for noting the reference error which has been corrected.

Hydrofluorocarbons (HFCs) have been introduced as replacements for ozone-depleting chlorofluorocarbons (CFCs) and hydrochlorofluorocarbons (HCFCs), for example, HFC-134a as a direct replacement for CFC-12. Conversely, HFC-23 is primarily an unavoidable by-product of chlorodifluoromethane HCFC-22 ($CHClF_2$) production due to the over-fluorination of chloroform ($CHCl_3$).

L75-91 This section is a rather abrupt change from the previous and could benefit from short introductory sentence or sub-heading. I would also suggest moving to after the next paragraph.

Reply. Introductory sentence has been added.

There have been a significant number of previously published papers related to HFC-23. Oram et al., (2008)……etc…

L88-91 I'm not sure why the extra details are relevant. Surprisingly, the reference to Simmonds et al., 2017, who reported HCFC-22 observations and emissions from the same network (and repeatedly discussed HFC-23), is missing, as are any other papers on HCFC-22.

Reply. Extra details have been removed as requested.

In addition we have moved lines 66-69 to a new paragraph (after line 90) and added the following text.

We have previously reported on the changing trends and emissions of HCFC-22 (Simmonds et al. 2017) and references therein.

L126-169 There are quite a lot of technical details in this section, which do not contribute to the main messages of the paper. These methods are also well established and I suggest moving large parts of the section to the supplement to improve readability.

Reply. We have moved the bulk of the methodology in Section 2 to the supplementary material, leaving only a brief description as follows-:

Ambient air measurements of HFC-23 and HCFC-22 at each site are recorded using the AGAGE GC-MS-Medusa instrument which employs an adsorbent-filled (HayeSep D) microtrap cooled to ~ -175^{o}C to pre-concentrate the analytes during sample collection of 2litres of air (Miller et al., 2008; Arnold et al., 2012). Samples are analysed approximately every 2 hours and are bracketed by measurements of quaternary standards to correct for short-term drifts in instrument response. Additional details of the analytical methodology are provided in the Supplementary material.

L203 I would be interested to know the methodology used to calculate this "liberal estimate". Is there a reference and could more information specifically on HFC-23 and HCFC-22 be given in the supplement?

Reply. As noted above this is a very subjective question, since we cannot really know something that we cannot measure. As we explain, we are nevertheless obliged to estimate absolute accuracy for modelling purposes and we have revised the paragraph in question in order to make these points more clearly.

Estimates of absolute accuracy are nevertheless needed for interpretive modelling applications, so despite the subjective nature of the question it is incumbent on those responsible for the measurements to provide an assessment of accuracy. Accordingly, we liberally estimate the absolute accuracies of these measurements as -3% to +2% for HFC-23 and ±1% for HCFC-22. The larger and asymmetric uncertainty for HFC-23 is due to its lower atmospheric and standard concentration, and to the lower stated purity of the HFC-23 reagent used to prepare the primary calibration scale, respectively.

L277 The annual growth probably relates to all of 2016, not just the end of that year?

Reply. Yes agreed and corrected

L293-296 The authors should make it clear that they have already published the HCFC22 data they refer to here.

Reply. Following text has been added.

These results are an update of our previously reported analysis of HCFC-22 (Simmonds et al., 2017).

L314-316 It is not clear whether this agrees with Carpenter and Reimann (2014) or not.

Reply. The text has been revised as follows:

These HFC-23 emissions estimates are slightly lower in 2006 and slightly higher in 2009 than the HFC-23 estimates of Miller et al, (2010) and Carpenter and Reimann, (2014).

L469 Please correct: un-abated.

Reply. Corrected.

L779-781 As published in Simmonds et al., 2017?

Reply.The following text has been added to the note for Table 3.

These HCFC-22 global emissions estimates are updates for HCFC-22 emissions reported in Simmonds et al. (2017)

L800-816 Missing from the two figures is previously published data and the respective sections of the manuscript would also benefit from a discussion of how mole fractions compare with published data. The axes on the inset of the first figure are very hard to read and the firn air is missing from the legend.

Reply. These two figures have been modified for additional clarity and the font size on the inset in Figure 1 has been increased. We previously discussed mole fractions in Section 3.2 and there is only a limited amount of additional reported observations of HFC-23 mixing ratios. We have added the following text to the introduction to include references to these limited observations.

Kim et al., (2010) reported HFC-23 measurements (November 2007-December 2008) at Jeju Island, Korea and also estimated regional atmospheric emissions. Most recently Fang et al., (2014, 2015) have provided top down estimates of HFC-23 emissions from China and East Asia and included observed HFC-23 mixing ratios at three stations Gosan, Korea, and Hateruma and Cape Ochi-ishi, Japan.